iScience

CellPress
OPEN ACCESS

Article

T Helper Plasticity Is Orchestrated by STAT3, Bcl6, and Blimp-1 Balancing Pathology and Protection in Malaria

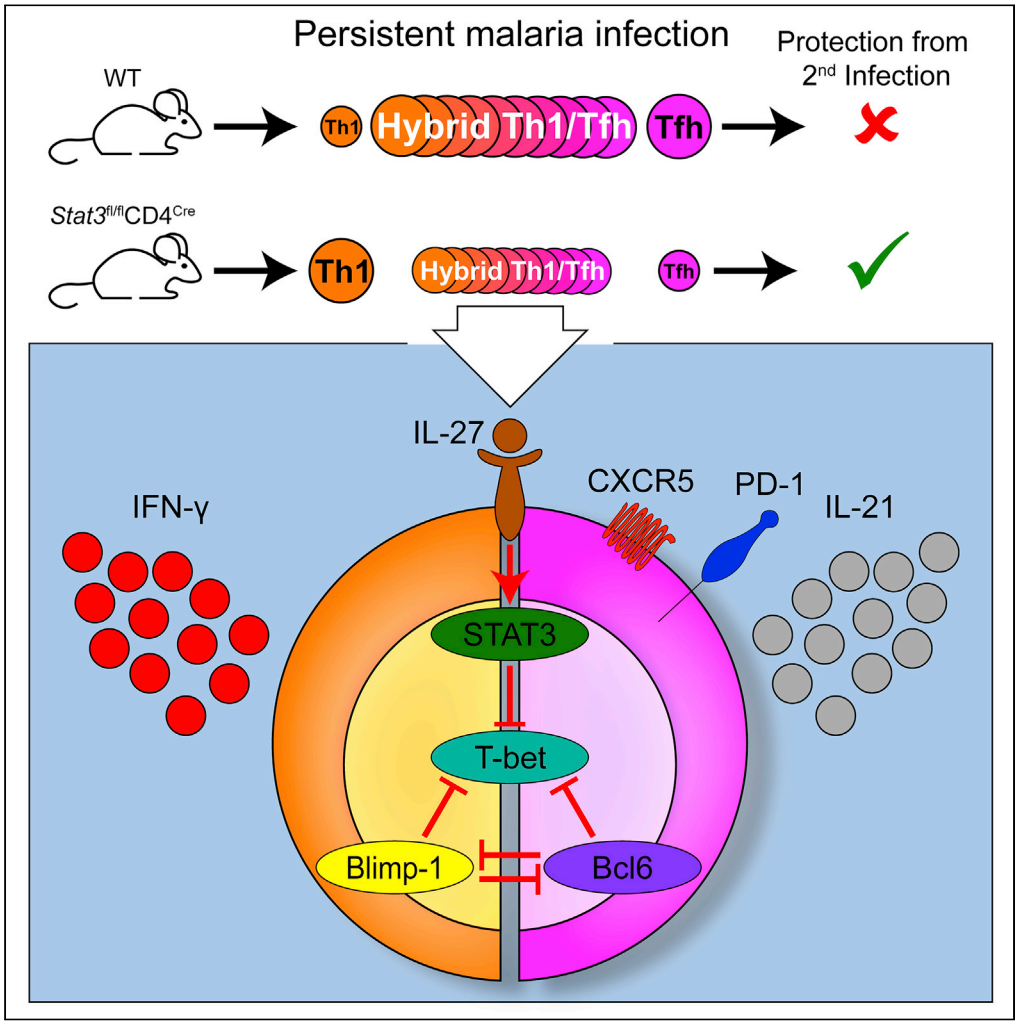

Victor H. Carpio, Florentin Aussenac, Lucinda Puebla-Clark, Kyle D. Wilson, Alejandro V. Villarino, Alexander L. Dent, Robin Stephens

rostephe@utmb.edu

HIGHLIGHTS

Plasmodium infection induces a CXCR5^{+}IFN-γ^{+}IL-21^{+} hybrid Th1/Tfh cell subset

STAT3/WSX-1, T-bet, Bcl6, and Blimp-1 regulate different aspects of Th1/Tfh phenotype

T cell-intrinsic STAT3 regulates degree of Th1 commitment of hybrid Th1/Tfh

Shifting the plastic response toward Th1-like cells promotes resistance from reinfection

Carpio et al., iScience *23*, 101310
July 24, 2020
https://doi.org/10.1016/j.isci.2020.101310

iScience

CellPress
OPEN ACCESS

Article

T Helper Plasticity Is Orchestrated by STAT3, Bcl6, and Blimp-1 Balancing Pathology and Protection in Malaria

Victor H. Carpio,[1] Florentin Aussenac,[2] Lucinda Puebla-Clark,[2] Kyle D. Wilson,[1] Alejandro V. Villarino,[3] Alexander L. Dent,[4] and Robin Stephens[1,2,5,*]

SUMMARY

Hybrid Th1/Tfh cells (IFN-γ^+IL-21$^+$CXCR5$^+$) predominate in response to several persistent infections. In *Plasmodium chabaudi* infection, IFN-γ^+ T cells control parasitemia, whereas antibody and IL-21$^+$Bcl6$^+$ T cells effect final clearance, suggesting an evolutionary driver for the hybrid population. We found that CD4-intrinsic Bcl6, Blimp-1, and STAT3 coordinately regulate expression of the Th1 master regulator T-bet, supporting plasticity of CD4 T cells. Bcl6 and Blimp-1 regulate CXCR5 levels, and T-bet, IL-27Rα, and STAT3 modulate cytokines in hybrid Th1/Tfh cells. Infected mice with STAT3 knockout (KO) T cells produced less antibody and more Th1-like IFN-γ^+IL-21$^-$CXCR5^{lo} effector and memory cells and were protected from re-infection. Conversely, T-bet KO mice had reduced Th1-bias upon re-infection and prolonged secondary parasitemia. Therefore, each feature of the CD4 T cell population phenotype is uniquely regulated in this persistent infection, and the cytokine profile of memory T cells can be modified to enhance the effectiveness of the secondary response.

INTRODUCTION

Both cellular and humoral responses are essential for immunity from *Plasmodium* infection. In humans, CD4 T cells that produce interferon (IFN)-γ in response to *Plasmodium falciparum* antigens accumulate with exposure, as do antibodies specific for each variant of parasite the host has been infected with, correlating with lower incidence of both parasitemia and hospitalization. A favorable ratio of interleukin (IL)-10 to tumor necrosis factor (TNF) correlates with resistance from pathology in both mice and people (Li et al., 2003; Luty et al., 1999; May et al., 2000), and CD4 T cells protect immunodeficient mice from dying of *Plasmodium chabaudi* infection (Stephens et al., 2005). Both IL-12 and IFN-γ, T helper-type 1 (Th1)-promoting cytokines, contribute to reduction of peak parasitemia by promoting parasite phagocytosis and generation of Th1-driven antibody isotypes (Su and Stevenson, 2000; Xu et al., 2000). IFN-γ production by T cells in response to *P. chabaudi* infection is initially strong, whereas it becomes downregulated as infection becomes controlled. Thereafter, a much reduced but recrudescent parasitemia is cleared by germinal center (GC)-derived antibody (Perez-Mazliah et al., 2017). IL-21, made predominantly by CXCR5$^+$ T cells, including T follicular helper (Tfh), is required for antibody isotype class switch and contributes significantly to full clearance (Carpio et al., 2015; Perez-Mazliah et al., 2015).

In *P. chabaudi* infection, we and others have shown that many cells express both IFN-γ and IL-21 (Carpio et al., 2015; Perez-Mazliah et al., 2015). IFN-γ^+IL-21$^+$ CD4 T cells also occur in chronic lymphocytic choriomeningitis virus (LCMV), tuberculosis, and *Listeria* infections (Elsaesser et al., 2009; Li et al., 2016; Tubo et al., 2013). *In vitro*, prolonged T cell receptor (TCR) signaling and IL-12 drive T cells from the Th1 to the Tfh phenotype (Fahey et al., 2011; Schulz et al., 2009; Tubo and Jenkins, 2014). CXCR5^{int} effector T cells (Teff) have been reported in other *Plasmodium* infections and can generate CXCR5^{hi}PD-1^{hi} GC Tfh cells in *Plasmodium berghei* (Ryg-Cornejo et al., 2016). Moreover, CXCR5^{int} Teff can help B cells make antibody, although less well than GC Tfh (Obeng-Adjei et al., 2015; Wikenheiser et al., 2018; Zander et al., 2017). We showed that the IFN-γ^+IL-21$^+$CXCR5$^+$ T cells in *P. chabaudi* infection express the Tfh markers ICOS and BTLA, along with the IFN-γ-induced chemokine receptor CXCR3, and the primary transcription factors of both Th1 and Tfh (T-bet and Bcl6) (Carpio et al., 2015). These data led us to the term "hybrid Th1/Tfh" to describe any IFN-γ^+ CD4 T cell also expressing IL-21 and/or CXCR5, functional markers

[1]Department of Microbiology and Immunology, University of Texas Medical Branch, Galveston, TX 77555-0435, USA

[2]Department of Internal Medicine, Division of Infectious Diseases, University of Texas Medical Branch, Galveston, TX 77555-0435, USA

[3]Molecular Immunology and Inflammation Branch, National Institute of Arthritis, Metabolic, and Skin Diseases, National Institutes of Health, Bethesda, MD 20892-1674, USA

[4]Department of Microbiology and Immunology, Indiana University School of Medicine, Indianapolis, IN 46202, USA

[5]Lead Contact

*Correspondence: rostephe@utmb.edu

https://doi.org/10.1016/j.isci.2020.101310

of Tfh. Strikingly, IFN-γ^+IL-21$^+$ T cells are also the main source of IL-10 (Carpio et al., 2015; Perez-Mazliah et al., 2015), a critical cytokine as it prevents lethal pathology in *P. chabaudi*-infected mice (Freitas do Rosario et al., 2012), and promotes antibody responses (Guthmiller et al., 2017). Hybrid Th1/Tfh cells also preferentially expand during *P. falciparum* infection, where they have been termed Th1-like Tfh (Obeng-Adjei et al., 2015). However, Bcl6-deficient T cells adoptively transferred into wild-type (WT) mice differentiated into both CXCR5^{int} and IFN-γ^+IL-21$^+$ T cells in *P. chabaudi* infection (Carpio et al., 2015), suggesting that these hybrid phenotype T cells are not of the Tfh lineage. The impaired ability of hybrid Th1/Tfh to help antibody production is likely due to an antagonism regulating Tfh effector functions through the network of STAT4 and T-bet expression and the effects of IL-2, IL-12, IFN-γ, and/or TNF, depending on the infection (Fang et al., 2018; Weinstein et al., 2018). In *P. berghei* ANKA infection, IFN-γ and/or TNF and T cell-intrinsic T-bet inhibit GC Tfh, GC B cell formation, and IgG production in response to infection (Ryg-Cornejo et al., 2016). Therefore, the hybrid Th1/Tfh population producing IFN-γ, IL-21, and IL-10 are likely to concurrently provide cellular protection and limit the large humoral response, which leads to hypergammaglobulinemia. It is not well understood which differentiation pathways control expression of these effector cytokines, particularly in persistent infections. Therefore, we have investigated the molecular regulation of T cell cytokine production and phenotype in response to infection with *Plasmodium spp.* through T cell-specific genetic manipulation to the test the importance of Th differentiation and plasticity *in vivo*.

Classically, committed IFN-γ^+ Th1 cells are generated by antigen stimulation in the presence of IL-12, which signals through STAT4 (Hsieh et al., 1993) which maximizes levels of the master regulator of Th1 differentiation, T-bet (Szabo et al., 2000). Th1 cells express CXCR3, but not CXCR5, which allows them to migrate away from the B cell follicle into the red pulp and inflamed tissues. Fully differentiated GC Tfh cells are identified as CXCR5^{hi}PD-1^{hi}, and their generation depends on the Tfh cell lineage-determinant transcription factor Bcl6 (Johnston et al., 2009; Nurieva et al., 2009). Many cytokines that regulate Tfh development, including IL-6, IL-27, and IL-21, signal through STAT3 (Crotty, 2014). IL-6 signaling through STAT3 secures Tfh programming by limiting Th1 differentiation (Choi et al., 2013). IL-27 signaling through STAT3 induces IL-21 production in T cells (Batten et al., 2010), which in turn promotes Tfh development (Nurieva et al., 2008). *In vitro* and in response to viral infection, STAT3-deficient T cells have a defect in Tfh differentiation (Ray et al., 2014), whereas humans with STAT3 dominant-negative mutations have compromised Tfh development (Ma et al., 2012). However, over the last few years, several lines of evidence suggest a complex regulation of Th1 and Tfh, where lineage determination is intertwined at the molecular level (Weinmann, 2014). For example, the transcription factor Blimp-1 can inhibit both Tfh and Th1 differentiation via transcriptional inhibition of Bcl6 and T-bet, respectively (Cimmino et al., 2008; Johnston et al., 2009). In the context of persistent infection, Blimp-1 also controls IL-10 production by Th1 cells (Parish et al., 2014). Therefore, we used an *in vivo* approach involving the most relevant transcription factors reported to date to understand the molecular regulation of T cells and protective responses to *Plasmodium spp.* infections.

Both Th1 and Tfh responses are critical for malaria immunity; however, the ideal balance between these T cell subsets remains unclear. Therefore, we investigated the roles of STAT3, T-bet, Bcl6, and Blimp-1 in the development of hybrid Th1/Tfh cells during persistent *P. chabaudi* infection to identify protective responses. We found that in contrast to the hybrid Th1/Tfh cells found in WT mice upon infection, T cells from T cell-specific STAT3-deficient mice (*Stat3*$^{fl/fl}$CD4^{Cre}, STAT3 TKO) preferentially differentiated into Th1 memory cells (IFN-γ^+IL-21$^-$T-bet^{hi}). Strikingly, STAT3 TKO mice were 100% protected from reinfection, whereas T-bet-deficient mice had no Th1 memory cells and higher parasitemia. Both mice had reduced serum levels of *Plasmodium*-specific IgG2b, the Th1 isotype, suggesting that the strong positive effect on parasitemia in STAT3 TKO mice was due to improved Th1 memory. Mechanistically, T-bet, and not STAT1 or STAT4, regulated IFN-γ production by T cells; and T cell-intrinsic expression of STAT3, Bcl6, and Blimp-1 each regulated T-bet expression during the peak of infection. Therefore, STAT3 is a key player regulating protection and the cytokine plasticity of memory T cells in malaria. These data support the hypothesis that Th cell pluripotency allows continued responsiveness promoting control of persistent infections and host homeostasis.

RESULTS

Plasmodium Infections Induce Hybrid Th1/Tfh and GC Tfh Cells

We have previously reported the presence of hybrid Th1/Tfh cells expressing both Tfh markers (CXCR5, ICOS, BTLA, IL-21, and Bcl6) and Th1 markers (CXCR3, IFN-γ, T-bet), as well as the regulatory cytokine

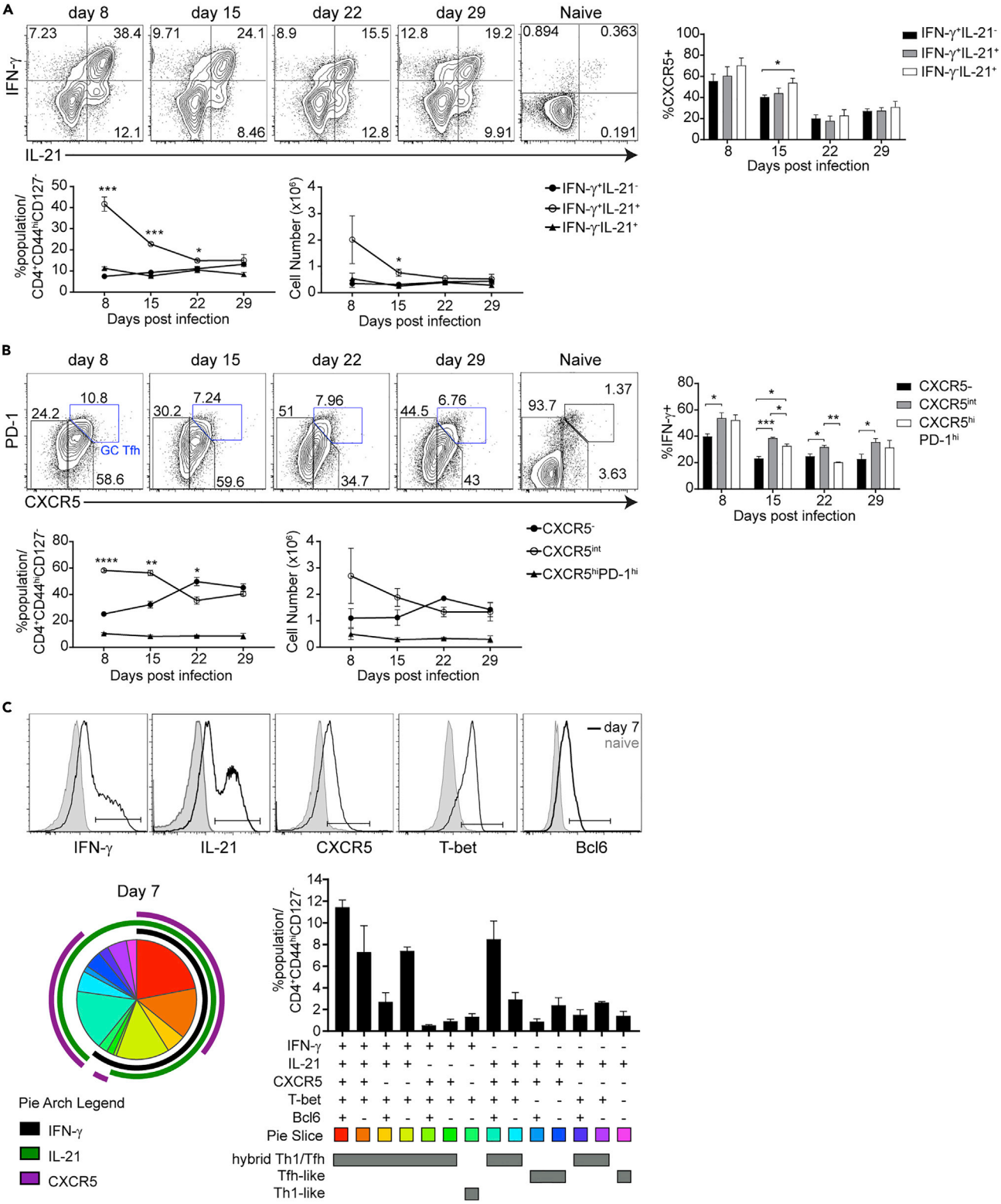

Figure 1. T Helper Differentiation during *P. chabaudi* Infection Resembles a Hybrid Th1/Tfh Phenotype

C57BL/6J mice were infected with *P. chabaudi* (10^5 iRBCs), and splenocytes were analyzed on the days post-infection indicated.

(A) Expression of IFN-γ and IL-21. Below, line graphs show percentage (left) and numbers (right) of IFN-γ^+IL-21^- (black filled dots), IFN-γ^+IL-21^+ (open circles), and IFN-γ^-IL-21^+ (filled triangles) Teff. Bar graph on the right shows CXCR5 expression in cytokine-producing populations.

Figure 1. *Continued*

(B) Expression of PD-1 and CXCR5 on CD4 Teff ($CD44^{hi}CD127^{-}$) and naive ($CD44^{lo}CD127^{+}$). Below, line graphs show percentage (left) and numbers (right) of $CXCR5^{-}$ (black filled dots), $CXCR5^{int}$ (open circles) Teff, and $CXCR5^{hi}PD\text{-}1^{hi}$ GC Tfh (filled triangles) populations. Bar graph on the right shows IFN-γ production by the different populations.

(C) Boolean gating of all possible combinations of IFN-γ, IL-21, CXCR5, T-bet, and Bcl6 expression of CD4 Teff on day 7 p.i. Top, histograms show gate marker used to define IFN-γ^{+}, IL-21^{+}, $CXCR5^{+}$, T-bet^{+}, and $Bcl6^{+}$ in CD4 Teff. Bottom left, pie chart shows the distribution of subsets. Bottom right, bar graph shows the percentage of the subsets.

Data representative of 3 experiments with 3 mice/group. Data are represented as mean ± SEM. * $p \leq 0.05$, ** $p \leq 0.001$, *** $p \leq 0.0001$, **** $p \leq 0.0001$. See also Figure S1.

IL-10 within effector T cells ($CD4^{+}CD44^{hi}CD127^{-}$) in *P. chabaudi* infection on day 7 post-infection (p.i.) (Carpio et al., 2015). Although hybrid Th1/Tfh cells have been described in several infections, including LCMV Clone 13 and tuberculosis, the timing of their generation has not been investigated to date. It is important to distinguish the hybrid Teff from GC Tfh, which are essential for GC formation. Therefore, we infected C57BL/6J mice with *P. chabaudi* (AS) or *P. yoelii* (17XNL) infected red blood cells (iRBCs, Figure S1A) and measured parasitemia. Using flow cytometry, we measured GC B cell numbers and the expression of CXCR5, PD-1, IFN-γ, IL-21, T-bet, and Bcl6 in Teff for the first 30 days of infection. We identified Th1-like cells as positive for only Th1 markers (IFN-$\gamma^{+}$and/or T-bet^{+}, but IL-$21^{-}$$CXCR5^{-}$), Tfh-like cells as positive for only Tfh markers (IL-$21^{+}CXCR5^{+/int}$, but IFN-$\gamma^{-}$and/or T-bet^{-}), and hybrid Th1/Tfh as cells that express any Th1, along with any Tfh marker. GC Tfh have been defined in the literature as ($CXCR5^{hi}PD\text{-}1^{hi}$), and we follow that convention throughout. GC B cells ($B220^{+}GL\text{-}7^{+}CD38^{lo}$) are highly visible in the third week of the response to both species. Unbiased t-distributed stochastic neighbor embedding analysis gated on $CD4^{+}$ T cells (Figure S1B) shows the small cluster of GC Tfh ($Bcl6^{hi}CXCR5^{hi}PD\text{-}1^{hi}$) and the larger islands of hybrid Th1/Tfh cells (IFN-γ^{+}IL-21^{+}) generated in response to both infections.

Throughout, we identify Teff as $CD44^{hi}CD127^{-}$, as IL-7Rα (CD127) is transiently downregulated upon activation, with negative expression in Teff on day 9 p.i. (Stephens and Langhorne, 2010). CD127 downregulation correlates with CD11a high expression (Figure S1C), which is upregulated by TCR, but not cytokine stimulation (McDermott and Varga, 2011), suggesting that $CD127^{-}$ is also a marker of TCR stimulation. In the first week of infection, the majority of Teff produce both IFN-γ and IL-21, averaging 41.67% of Teff in *P. chabaudi* and 48.57% in *P. yoelii* in the first week of infection (Figures 1A and S1D). The IFN-γ^{+}IL-21^{+} Teff population decreases by half in the second week and then has a stable presence. In addition, there is an increase of CXCR5 expression on Teff in response to both *P. chabaudi* and *P. yoelii* (Figures 1B and S1E). GC Tfh cells are present in stable numbers starting in the first week in both infections, as previously suggested (Wikenheiser et al., 2016). Boolean gating analysis using IFN-γ, IL-21, CXCR5, T-bet, and Bcl6 at day 7 p.i. showed that 66.43% Teff from *P. chabaudi*-infected mice co-express IFN-γ^{+} and at least one marker of Tfh (IL-21, Bcl6, or CXCR5), with IL-21^{+}IFN-γ^{+} included in the majority of those sub-populations (Figures 1C and S1F). The other population represented at over 4% of Teff is positive for all markers, including T-bet, but not IFN-γ. On the other hand, the IFN-γ^{+}T-bet^{+} Th1-like cells represent a modest fraction (2.91%) of the response. Therefore, infection with *Plasmodium spp.* drives generation of a large population of IFN-γ^{+}IL-21^{+} hybrid Th1/Tfh effector cells, which peak in the first week, as well as GC Tfh that are more stably represented, but very few IFN-γ^{+} Th1-like cells without Tfh markers. These IFN-γ^{+}IL-21^{+} hybrid Th1/Tfh cells are reminiscent of CD4 T cells identified in other persistent infections (Crawford et al., 2014), leading us to investigate the role of continuing infection in their generation, and to identify molecular mechanisms regulating their generation.

Shorter Infection Results in Fewer Hybrid Th1/Tfh Cells

Hybrid Th1/Tfh cells have been documented in human patients with malaria (Obeng-Adjei et al., 2015) and in other persistent infections including LCMV Clone 13 (Crawford et al., 2014; Nakayamada et al., 2011) using various combinations of Th1 and Tfh markers. On the other hand, acute infections can promote independent differentiation of Th1 and Tfh populations (Curtis et al., 2010; Hale et al., 2013). We have previously shown that complete parasite clearance by the antimalarial drug mefloquine (MQ) given starting on day 3 p.i. increased the Tcm/Tem ratio in the memory phase compared with persistently infected animals (Opata et al., 2015). As no qualitative change in phenotype was observed when drug treatment began on day 5 or 30 p.i., there seems to be a limited window for determining the quality of T cell priming. As Tcm and Tfh generation seems to be linked (Pepper et al., 2011), we tested if limiting the duration of infection by drug treatment would alter the T cell cytokine profile away from IFN-γ^{+}IL-21^{+} hybrid Th1/Tfh. MQ treatment of *P. chabaudi*-infected animals starting on day 3 cleared infection almost completely by day 5

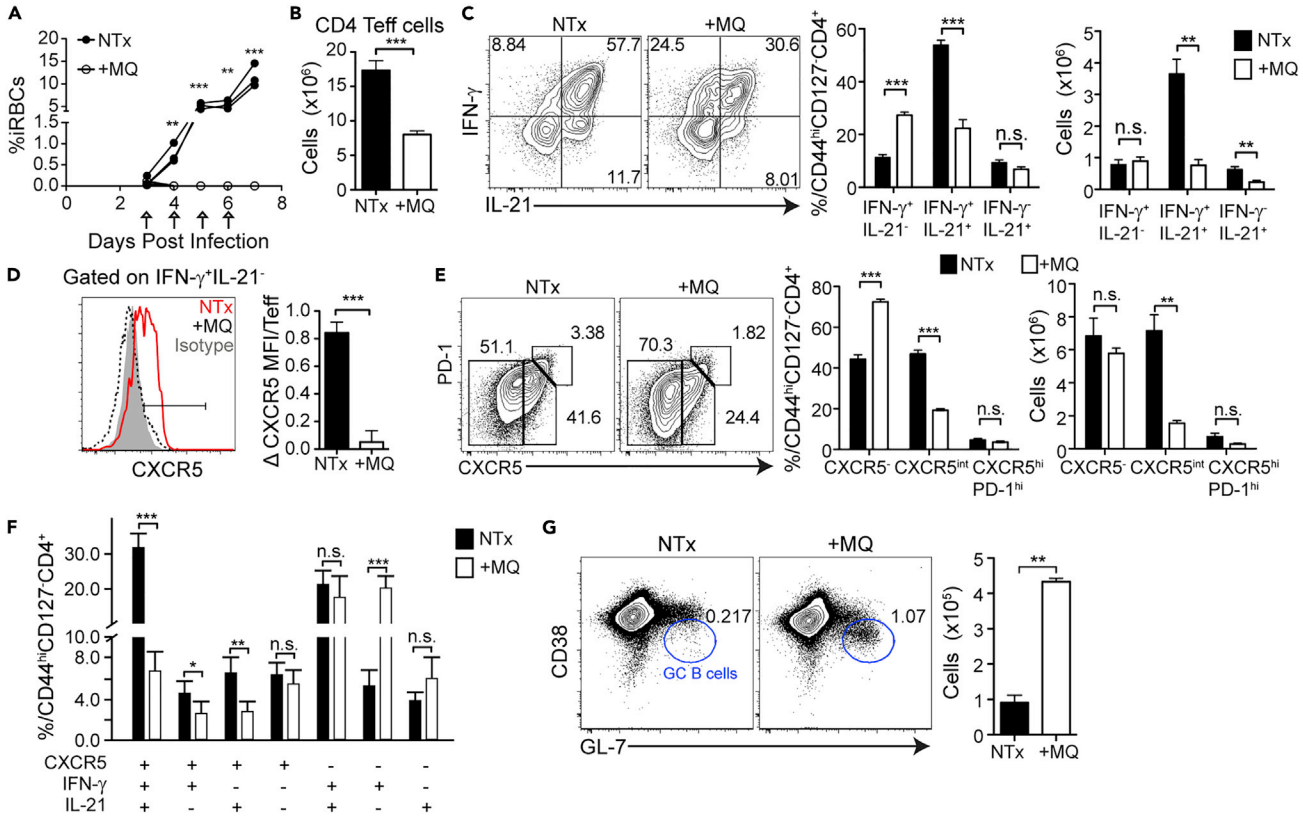

Figure 2. Drug-Cured Mice Have Fewer IFN-γ$^+$IL-21$^+$CXCR5$^+$ Hybrid Th1/Tfh and More IFN-γ$^+$IL-21$^-$CXCR5$^-$ Th1-Like Cells

C57BL/6J mice were infected, one group was treated with anti-malarial drug mefloquine (MQ) by oral gavage starting day 3 p.i. and splenocytes analyzed at day 7 p.i.

(A) Parasitemia in treated (+MQ, open circles) and not-treated (NTx, black filled circles) groups. Arrows indicate MQ treatment.

(B, C, and E) (B) CD4 Teff numbers in +MQ (white bar) and NTx (black bar). (C) Expression of IFN-γ and IL-21 and (E) PD-1 and CXCR5 in Teff. Bar graphs show percentages and numbers of Teff subsets.

(D) Histogram overlay shows CXCR5 expression in Th1-like IFN-γ$^+$IL-21$^-$ Teff. Bar graph shows fold change of CXCR5 mean fluorescence intensity (MFI) over isotype control.

(F) Boolean gating analysis of CXCR5$^+$, IFN-γ$^+$, and IL-21$^+$ expression by Teff.

(G) Expression of CD38 and GL-7 on B cells (gated on B220$^+$MHCII$^+$). Bar graph shows numbers of GC B cells (CD38^{lo}GL7$^+$) per spleen.

Data representative of 3 experiments with 3–4 mice/group. Data are represented as mean ± SEM. * p <0.05, ** p <0.01, *** p <0.001, **** p <0.0001, n.s., not significant. See also Figure S2.

(Figure 2A). MQ treatment has no known effect on immune cells at this low dose (Paivandy et al., 2014). Stopping the infection early (+MQ) decreased the numbers of Teff (Figure 2B). In addition, there were also striking qualitative changes. MQ-treated animals had a higher fraction of Th1-like IFN-γ$^+$IL-21$^-$ Teff, and a strong reduction in the fraction and number of IFN-γ$^+$IL-21$^+$ T cells (Figure 2C). These IFN-γ$^+$IL-21$^-$ Teff also did not express more CXCR5 than naive T cells, unlike the Th1-like cells in persistent *P. chabaudi* (Figure 2D). In fact, treatment of infection significantly reduced the proportions of all CXCR5^{int} cells in the Teff population at day 7 p.i. (Figure 2E). Examining all markers together, MQ treatment reduced the proportion of IFN-γ$^+$IL-21$^+$CXCR5$^+$ by 79.33% ± 3.41%, but not IFN-γ$^+$IL-21$^+$CXCR5$^-$, and increased the proportions of Th1-like IFN-γ$^+$CXCR5$^-$IL-21$^-$ compared with untreated animals (Figure 2F), suggesting that generation of CXCR5$^-$ Th1-like cells is inhibited by infection lasting longer than 3 days. To investigate any potential role of hybrid Th1/Tfh in early GC formation, we measured GC B cells on day 7, the day of peak T-bet expression in T cells. GC B cell numbers were increased at day 7 p.i. in treated compared with untreated mice (Figure 2G), opposite to hybrid Th1/Tfh cells. The untreated mice also showed a distinct population of CD38^{hi}GL-7$^+$ B cells, which has been previously described as GC-independent memory B cell precursors (Taylor et al., 2012). In contrast, starting treatment on day 5 rather than day 3 reduced infection immediately (Figure S2A), but had no effect on the fraction of IFN-γ$^+$IL-21$^+$ (Figure S2B) or CXCR5^{int} Teff (Figure S2C). T cell priming occurs before day 5 of *P. chabaudi* infection (Opata et al.,

2015; Sponaas et al., 2012). Therefore, we conclude that the cytokine milieu surrounding antigen presentation regulates priming of the hybrid Th1/Tfh cell phenotype. However, the transcriptional mechanisms regulating this new phenotype are not clear.

T-bet Regulates IFN-γ and IL-21 Production by Hybrid Th1/Tfh Cells

Th1 cells play a crucial role in immunopathogenesis and host survival in *Plasmodium spp*. infection (Oakley et al., 2013; Su and Stevenson, 2000). Basal levels of T-bet expression can be driven by TCR signaling, IFN-γ, and STAT1. T-bet then upregulates IL-12Rβ2, promoting IL-12 signaling through STAT4, to drive increased T-bet expression and full Th1 commitment (Afkarian et al., 2002; Szabo et al., 2000). Interestingly, T-bet has been shown to work in concert with Bcl6 to regulate the plasticity of Th1 cells (Oestreich et al., 2012). Although we have observed very few T-bet^{hi} Th1 committed cells in our studies, most Teff express T-bet at a low level (Carpio et al., 2015). The role of Th1 transcriptional activators in *P. chabaudi* infection has not been well established, particularly in the differentiation of hybrid Th1/Tfh cells. Using *P. chabaudi*-infected mutant mice, we found that STAT4 was not required for the generation of IFN-γ$^+$IL-21$^+$ Teff (Figure S3A), but it was critical for GC Tfh differentiation (Figure S3B). Although surprising, this agrees with recent reports showing a role for STAT4 in generating GC Tfh in infection (Weinstein et al., 2018). T cell-intrinsic STAT1 was not required for generation of IFN-γ$^+$IL-21$^+$ T cells as well (Figure S3C). T-bet-deficient (*tbx21*$^{-/-}$, T-bet knockout (KO)) mice infected with *P. chabaudi* had a strong reduction in IFN-γ production and a significant increase in the fraction and number of IL-21$^+$IFN-γ$^-$ Tfh-like cells (Figure 3A). The overall percentage of IL-21$^+$ Teff in WT mice was 38.33% ± 1.77%, whereas in KO mice was 52.93% ± 2.38% (p = 0.008), suggesting a role for T-bet in IL-21 production. In addition, there was a large decrease in the overall numbers of *tbx21*$^{-/-}$ Teff compared with WT on day 7 p.i. (Figure 3B). T-bet deficiency increased the level of expression of CXCR5 on Teff but had no effect on the relative fraction of GC Tfh (Figure 3C). Boolean gating analysis revealed a reduction in hybrid IFN-γ$^+$IL-21$^+$CXCR5$^+$ cells and a shift toward more Tfh-like Teff (IFN-γ$^-$IL-21$^+$CXCR5$^{+/-}$) in the absence of T-bet (Figure 3D). However, we did not identify a significant change in the number of GC B cells at day 7 p.i. (Figure 3E). Supporting an important role for IFN-γ$^+$ Teff and T-bet$^+$ B cells in control of this infection, 40% of T-bet KO mice died from infection (Figure S3D). T-bet KO mice that survived the infection did not control parasitemia as well as WT (Figure S3E) and had worse weight loss and hypothermia (Figure S3F). These data suggest that T-bet regulates IFN-γ and IL-21 production by hybrid Th1/Tfh cells. Moreover, T-bet expression is required for control of parasitemia and immunopathology in *P. chabaudi* infection.

Bcl6 and Blimp-1 Regulate CXCR5 Levels in *P. chabaudi* Infection

The major Tfh regulatory transcription factor, Bcl6 can bind T-bet and inhibit its function (Oestreich et al., 2012), and indeed, we previously reported that Bcl6 levels correlate with the level of *ifng* transcription in Teff in *P. chabaudi* (Carpio et al., 2015). To test the role of Bcl6 in the differentiation of hybrid Th1/Tfh, we infected *Bcl6*$^{fl/fl}$CD4^{Cre} (Bcl6 TKO) and *Bcl6*$^{fl/fl}$ (WT) mice with *P. chabaudi*. The percentage of IFN-γ$^+$IL-21$^+$ Teff did not change in the Bcl6 TKO mice on day 7 p.i, although IFN-γ$^-$IL-21$^+$ and overall Teff numbers were reduced (Figure 4A). As expected, *bcl6*$^{-/-}$ Teff did not generate GC Tfh (Figure 4B). Interestingly, the proportion and numbers of CXCR5$^+$ Teff decreased at day 7 p.i. on *bcl6*$^{-/-}$ Teff. Overall, Bcl6 deficiency resulted in an average 65% reduction of CXCR5$^+$IL-21$^+$IFN-γ$^-$ Tfh-like fraction (Figure 4C). We confirmed that T cell-specific Bcl6 deficiency had an effect only on parasite clearance (Figure S4A, Perez-Mazliah et al., 2017) and a slight increase in IL-10 in T cells (data not shown).

In CD4 T cells, Blimp-1 can inhibit both T-bet and Bcl6 and is known to promote IL-10 production in *P. chabaudi* (Cimmino et al., 2008; Montes de Oca et al., 2016). We also tested the role of Blimp-1, the reciprocal regulator of Bcl6 (Johnston et al., 2009), infecting *Prdm1*$^{fl/fl}$CD4^{Cre} (Blimp-1 TKO) animals. We found modest differences in cytokine production (Figure 4D). However, the percentage, but not the number, of CXCR5$^+$ Teff was increased in *prdm1*$^{-/-}$ Teff due to a shift in mean fluorescence intensity (Figure 4E). Boolean analysis revealed that the relative fraction of IFN-γ$^+$IL-21$^+$CXCR5$^+$ hybrid Th1/Tfh was also increased, whereas Th1 IFN-γ$^+$IL-21$^-$CXCR5$^-$ cells decreased in infected Blimp-1 TKO animals (Figure 4F). Despite equal parasite levels, all the Blimp-1 TKO mice died, similar to IL-10 KO mice (Figure S4B). In summary, Bcl6 and Blimp-1 coordinately regulate CXCR5 (and IL-10) expression levels in hybrid Th1/Tfh cells.

Effector T Cells Deficient in STAT3 Become More Th1-like Cells

Because STAT3 promotes the Tfh phenotype (Batten et al., 2010; Choi et al., 2013; Nurieva et al., 2008; Ray et al., 2014), we hypothesized that STAT3 could also be a transcriptional regulator of the phenotype and/or function of

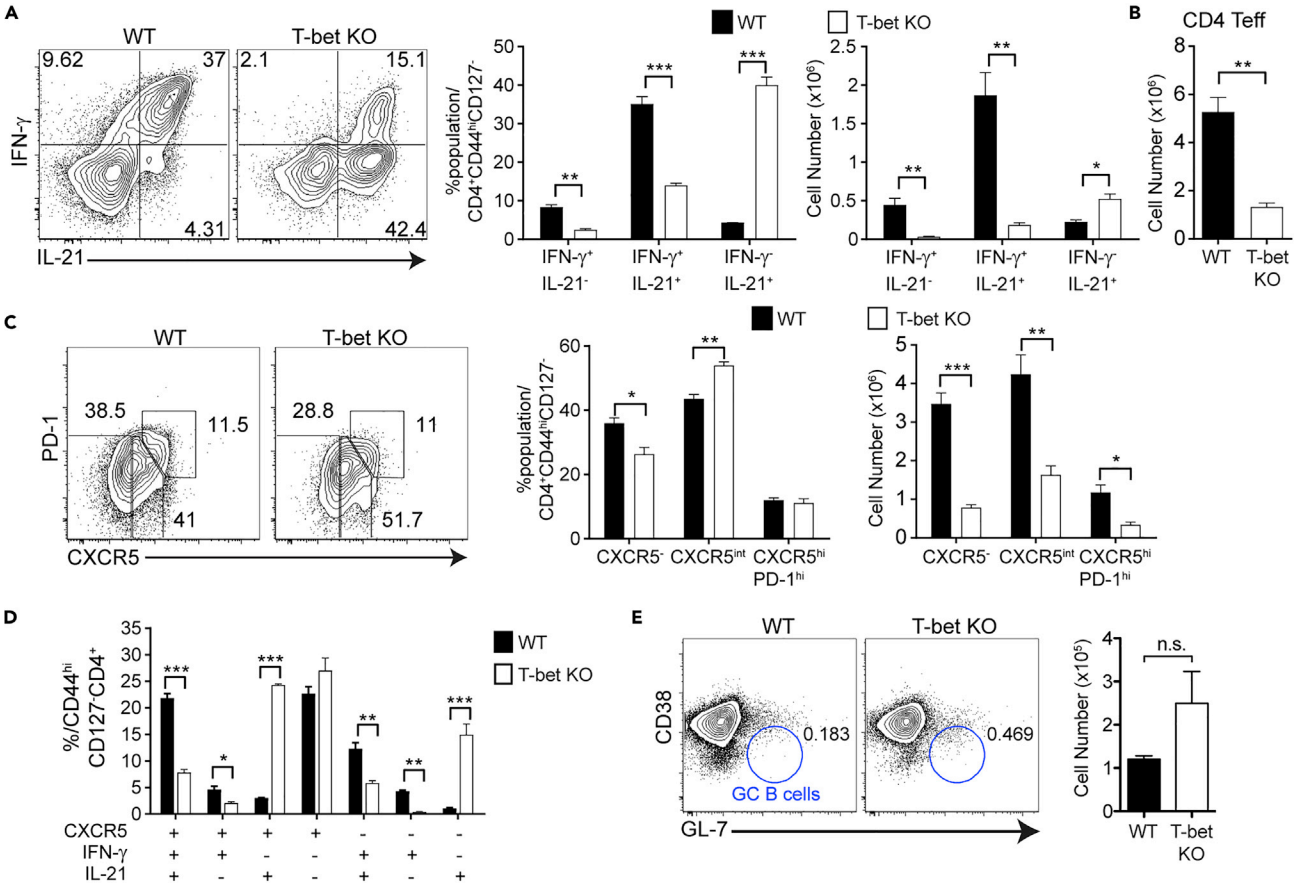

Figure 3. T-bet Deficiency Reduces IFN-γ$^+$IL-21$^+$CXCR5$^+$ Hybrid Teff and Th1 but Promotes IFN-γ$^-$IL-21$^+$ T Helper Differentiation in *P. chabaudi* Infection

T-bet KO and WT animals were infected, and splenocytes were analyzed at day 8 p.i.

(A) Expression of IFN-γ and IL-21 in Teff. Bar graphs show percentages and numbers in WT (black bars) and T-bet KO (white bars).

(B) Bar graph shows CD4 Teff numbers.

(C and D) (C) Expression of PD-1 and CXCR5 in Teff. (D) Boolean analysis of CXCR5$^+$, IFN-γ$^+$, and IL-21$^+$ within WT and T-bet KO Teff.

(E) CD38 and GL-7 in B cells (B220$^+$MHCII$^+$). Bar graph shows numbers of GC B cells (CD38^{lo}GL7$^+$).

Data representative of 2 experiments, 3–8 mice/group. Data are represented as mean ± SEM. * p <0.05, ** p <0.01, *** p <0.001, **** p >0.05, n.s, not significant. See also Figure S3.

hybrid Th1/Tfh cells. To test this hypothesis, we infected *Stat3*$^{fl/fl}$CD4^{Cre} (STAT3 TKO) and *Stat3*$^{fl/fl}$ (WT) animals with *P. chabaudi* or *P. yoelii* and analyzed splenocytes at day 7 or 10 p.i, respectively, by flow cytometry. STAT3 TKO mice infected with *P. chabaudi* showed a decrease in the percentage of IFN-γ$^+$IL-21$^+$ Teff, whereas the opposite was true for mice infected with *P. yoelii* (Figures 5A and S5A). We found no significant differences in the proportions of GC Tfh in either infection model (Figures 5B and S5B). However, using Boolean gating it became clear that STAT3 TKO mice infected with either *P. chabaudi* or *P. yoelii* both showed a reduction in the percentage of hybrid Th1/Tfh cells (IFN-γ$^+$IL-21$^+$CXCR5$^+$, Figures 5C and S5C). There was a concomitant increase in the fraction of Th1-like cells (IFN-γ$^+$IL-21$^-$CXCR5$^-$) in STAT3 TKO, and some small differences in the individual markers. In both infections, STAT3 TKO mice also had a significant reduction in IFN-γ$^-$IL-21$^+$ Teff, supporting reports that STAT3 signaling promotes IL-21 expression. Moreover, STAT3 TKO mice had an increase in the more Th1-like CXCR5$^{int/lo}$T-bet^{hi} population compared with the two apparently separable populations seen in WT (Figures 5D and S5D). We interpret these data to suggest a continuum of plastic hybrid Th1/Tfh cells from a Th1-like to Tfh-like bias, rather than separate or terminally differentiated subsets. This would predict that cytokines that signal through STAT3 could shift the hybrid population over the course of infection. To test this, we blocked IL-6 and IL-27 signaling. Both cytokines signal through STAT3 and can influence Tfh and Th1 differentiation in other models (Batten et al., 2010; Sebina et al., 2017). Neutralization of IL-6 during infection of WT animals did not change the hybrid Th1/Tfh phenotype (Figure S6A). However, when T cells deficient in

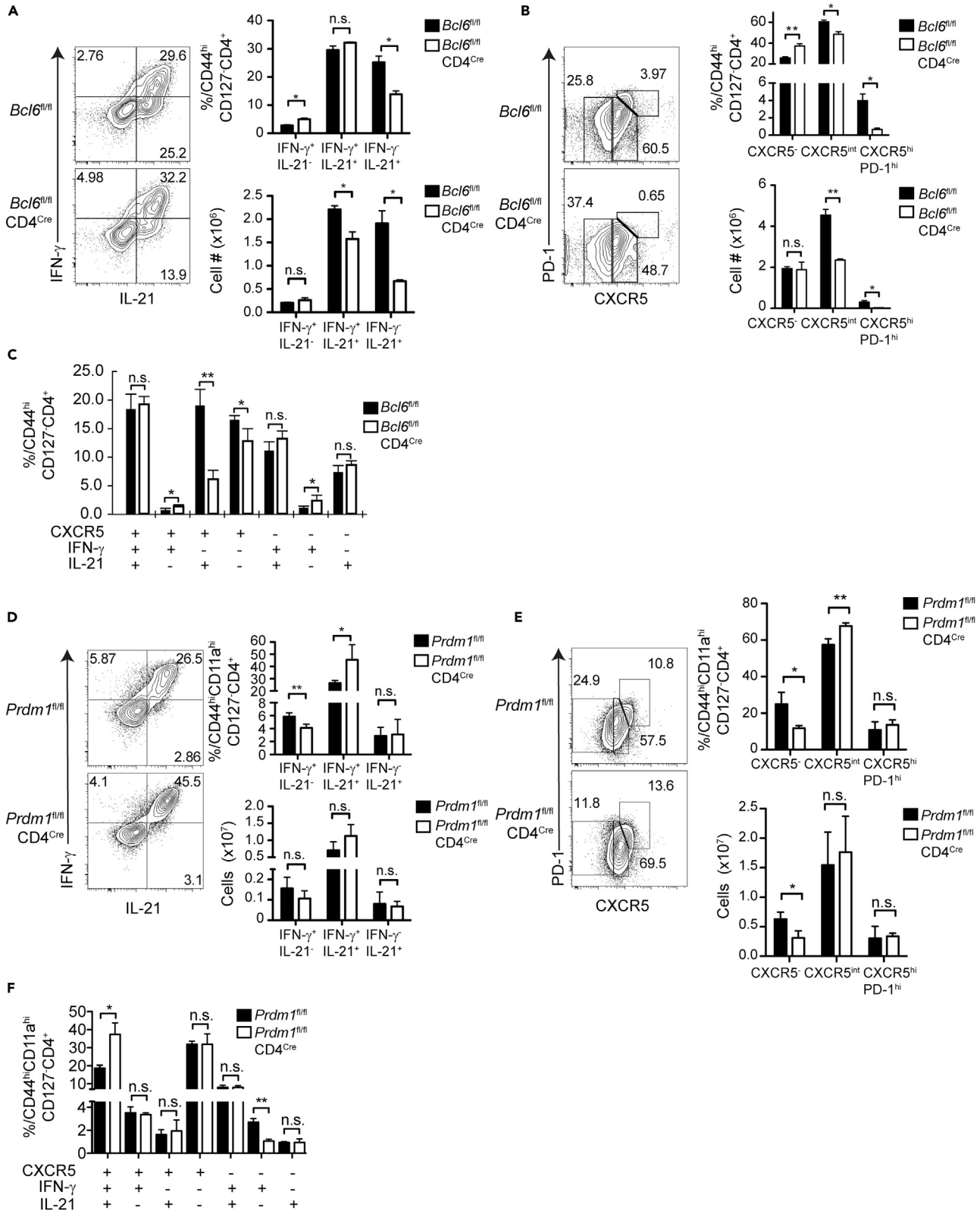
A
Bcl6fl/fl
Bcl6fl/fl CD4Cre
IFN-γ
IL-21
2.76
29.6
25.2
4.98
32.2
13.9
%/CD44hi CD127-CD4+
Cell # (x10^6)
IFN-γ+ IL-21-
IFN-γ+ IL-21+
IFN-γ- IL-21+
n.s.
B
PD-1
CXCR5
25.8
3.97
60.5
37.4
0.65
48.7
CXCR5- CXCR5int CXCR5hi PD-1hi
C
CXCR5
IFN-γ
IL-21
D
Prdm1fl/fl
Prdm1fl/fl CD4Cre
%/CD44hiCD11ahi CD127-CD4+
Cells (x10^7)
5.87
26.5
2.86
4.1
45.5
3.1
E
10.8
24.9
57.5
13.6
11.8
69.5
F

Figure 4. Roles of Bcl6 and Blimp in T Cell Differentiation during *P. chabaudi* Infection

(A–C) *Bcl6*$^{fl/fl}$CD4^{Cre} (TKO) and *Bcl6*$^{fl/fl}$ (WT) animals were infected, and splenocytes were analyzed at day 7 p.i. Contour plots and bar graphs show expression of (A) IFN-γ/IL-21 or (B) PD-1/CXCR5 gated on Teff. (C) Boolean analysis of CXCR5$^+$, IFN-γ$^+$, and IL-21$^+$ subsets within WT (black bar) and Bcl6 TKO (white bar) Teff.

(D–F) *Prdm11*$^{fl/fl}$CD4^{Cre} (Blimp-1 TKO) and *Prdm11*$^{fl/fl}$ (WT) animals were infected and splenocytes were analyzed at day 7 p.i. Contour plots and bar graphs show subsets of (D) IFN-γ/IL-21 or (E) PD-1/CXCR5 gated on Teff. (F) Boolean analysis of CXCR5$^+$, IFN-γ$^+$, and IL-21$^+$ within WT (black bars) and Blimp-1 TKO (white bars) Teff.

Data representative of 3 experiments, 3–4 mice/group. Data are represented as mean ± SEM. * p <0.05, ** p <0.01, n.s. p >0.05, not significant. See also Figure S4.

WSX-1 (IL-27Rα) were transferred into congenically marked recipients, which were then infected, the resulting divided Teff population (CD4$^+$CTV$^-$) contained more IFN-γ$^+$IL-21$^-$ Th1-like cells compared with WT donor cells (Figure S6B). This suggests that IL-27 is responsible for promoting IL-21 expression in IFN-γ$^+$ T cells in *P. chabaudi* infection. IL-27Rα deficiency in T cells also strongly reduced GC Tfh but did not affect CXCR5^{int} T cells. Generation of *P. chabaudi*-specific antibody was also affected by STAT3 deficiency in T cells. IgG titers were significantly less at day 35 p.i. in STAT3 TKO mice, whereas the relative concentration of IgM was not affected (Figure 5E). In addition, the proportion of GC B cells was significantly reduced in STAT3 TKO mice at days 20 and 55 p.i. (Figure 5F, d55 not shown). *P. chabaudi*-infected STAT3 TKO mice had consistently prolonged parasitemia (Figure S6C) and pathology (Figure S6D). However, no STAT3 TKO mice died of *P. chabaudi* infection (n = 40). These results indicate that STAT3 regulates the phenotype and cytokine production of hybrid Th1/Tfh cells during *Plasmodium* infection through IL-27Rα signaling. However, STAT3 deficiency is detrimental for parasite control, prolonging pathology in the first infection.

T-bet Expression Is Regulated by Bcl6, Blimp-1 and STAT3

Based on the strong effect of T-bet deletion on IFN-γ production, we hypothesized that T-bet regulation could modulate the pathogenic potential of T cells *in vivo*. We previously showed that T-bet is downregulated from day 7 to day 9 p.i., even though day 9 is the peak of IFN-γ$^+$ Teff numbers (Carpio et al., 2015). Therefore, we measured T-bet expression in all the TKO mice previously described. In Bcl6 TKO animals, T-bet expression was maintained at intermediate levels in Teff from day 7 to day 9 p.i., suggesting Bcl6 controls T-bet expression at the peak of infection (Figure 6A). Blimp-1 expression was also increased at day 9 p.i. in Bcl6 TKO. *Prdm1*$^{-/-}$ Teff showed an increase in the expression of T-bet, as well as in Bcl6, at day 7 p.i. (Figure 6B). STAT3 TKO Teff also had more T-bet and Blimp-1 expression at day 7 p.i. (Figure 6C). Bcl6 expression was not affected in STAT3 TKO Teff in *P. chabaudi* infection; however, it was reduced on day 10 p.i. of *P. yoelii* infection of STAT3 TKO (Figure S5F). In conclusion, Bcl6, Blimp-1, and STAT3 work in concert to regulate the expression of T-bet, IFN-γ, CXCR5, and each other, in Teff during persistent *Plasmodium* infection.

As the hybrid Th1/Tfh phenotype is increased when infection lasts longer than 3 days, we investigated the functional phenotype of Teff in TKO mice during shorter infection. WT and TKO animals were infected, and one group of each was treated with MQ starting at day 3 p.i. (Figure S7). Data are quantified as a ratio of TKO over WT to illustrate the degree of the effect of removal of each transcription factor in the longer (NTx) or the shorter (+MQ) infection. Both Th1-like IFN-γ$^+$IL-21$^-$ and hybrid IFN-γ$^+$IL-21$^+$ Teff were significantly increased in the short-term infection in Bcl6 TKO mice compared with WT, showing a larger effect of Bcl6 on IFN-γ expression in shorter stimulation than longer (Figure S7A). Blimp-1 plays a larger role in longer infection, as only untreated infected Blimp-1 TKO (NTx), but not treated, had fewer IFN-γ$^+$IL-21$^-$ with a concomitant increase in hybrid IFN-γ$^+$IL-21$^+$, supporting its role in IL-10 expression. On the other hand, STAT3 regulates IFN-γ in both long and short infections. This is clearly shown in the strong increase of IFN-γ$^+$IL-21$^-$ Teff in STAT3 TKO mice compared with WT. Strikingly, GC Tfh generation was only affected by STAT3 deficiency in the shortened infection, supporting the previously described role of STAT3 in Tfh in acute infection (Figure S7B, Ray et al., 2014). Together, these results suggest that the role of each transcription factor is dependent on the duration of strong priming, presumably due to differential expression of cytokines and transcription factors driven by the milieu.

Increasing Th1 Bias in Memory T Cells Correlates with Lower Parasitemia in Reinfection

Th type-1 cytokines have a strong impact on parasitemia in mice and humans (Luty et al., 1999; Su and Stevenson, 2000), although less is known about re-infection. Given the increase of Th1 cells and effective clearance of persistent parasite in STAT3 TKO mice, we re-infected STAT3 TKO animals to test for immunity (Figure 7). To ensure parasite clearance after the first infection in both STAT3 TKO and WT, we treated

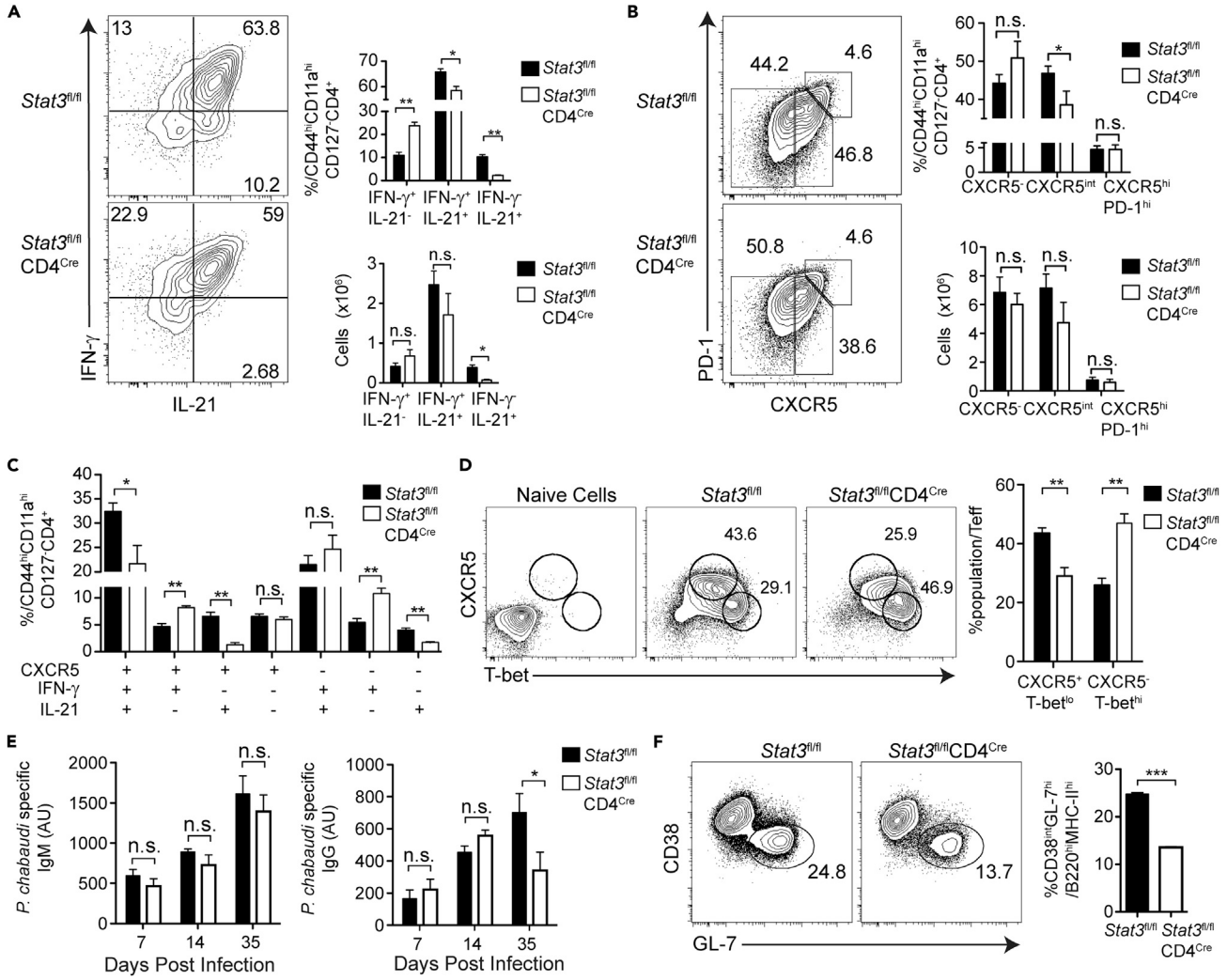

Figure 5. STAT3 Deficiency Reduces IFN-γ$^+$IL-21$^+$CXCR5$^+$ Hybrid Teff and Increases Th1 Bias in *P. chabaudi* Infection

(A and B) *Stat3*$^{fl/fl}$CD4^{Cre} (TKO) and *Stat3*$^{fl/fl}$ (WT) animals were infected, and splenocytes were analyzed at day 7 p.i. Expression of (A) IFN-γ and IL-21 and (B) PD-1 and CXCR5 in Teff. Bar graphs show percentages and numbers of subsets.

(C) Boolean analysis of CXCR5$^+$, IFN-γ$^+$, and IL-21$^+$ within WT (black bars) and STAT3 TKO (white bars) Teff.

(D) Expression of CXCR5 and T-bet in Teff. Bar graph shows percentages Tfh-like (CXCR5$^+$T-bet^{lo}) and Th1-like (CXCR5$^-$T-bet^{hi}) subsets.

(E) Bar graphs showing *P. chabaudi*-specific IgM (left) and IgG (right) from serum d35 p.i.

(F) Expression of CD38 and GL-7 in B cells (B220$^+$MHCII$^+$) day 20 p.i. Bar graph shows numbers of GC B cells (CD38^{lo}GL7$^+$).

Data representative of 3 experiments, 3–4 mice/group. Data are represented as mean ± SEM. * p <0.05, ** p <0.01, *** p <0.001, **** p >0.05, n.s, not significant. See also Figures S5 and S6.

with the anti-malarial drug chloroquine (CQ), which effectively eliminates low levels of *P. chabaudi* parasitemia (Hunt et al., 2004). STAT3 TKO mice controlled a high-dose second challenge (1 × 10^7 iRBCs) completely, with infection becoming undetectable by day 3 post-reinfection (p.r.i, Figure 7A). WT mice showed significantly higher parasitemia that peaked around day 4 and was controlled by day 7 p.r.i. The proportion of IFN-γ$^+$IL-21$^-$ T cells was higher in STAT3 TKO mice at day 7 p.r.i, and the numbers of IFN-γ$^+$IL-21$^+$ Teff were less (Figure 7B). The numbers of both GC Tfh (Figure 7C) and GC B cells (Figure 7D) were significantly less in STAT3 TKO mice than WT at day 7 p.r.i. Importantly, the levels of *P. chabaudi*-specific IgG and Th1-driven isotype, IgG2b, were significantly less in STAT3 TKO mice than WT (Figure 7E). To determine if increased Th1 bias in the *stat3*$^{-/-}$ Teff observed during the first infection was maintained into the memory phase, we analyzed antigen-experienced memory T cells (Tmem, CD11a^{hi}CD49d^{hi} CD44^{hi}CD127^{hi}) at day 55 p.i. Indeed, STAT3-deficient Tmem had higher percentages of IFN-γ$^+$IL-21$^-$ Th1-like cells (Figure 7F) and maintained higher expression of T-bet (Figure 7G) than WT.

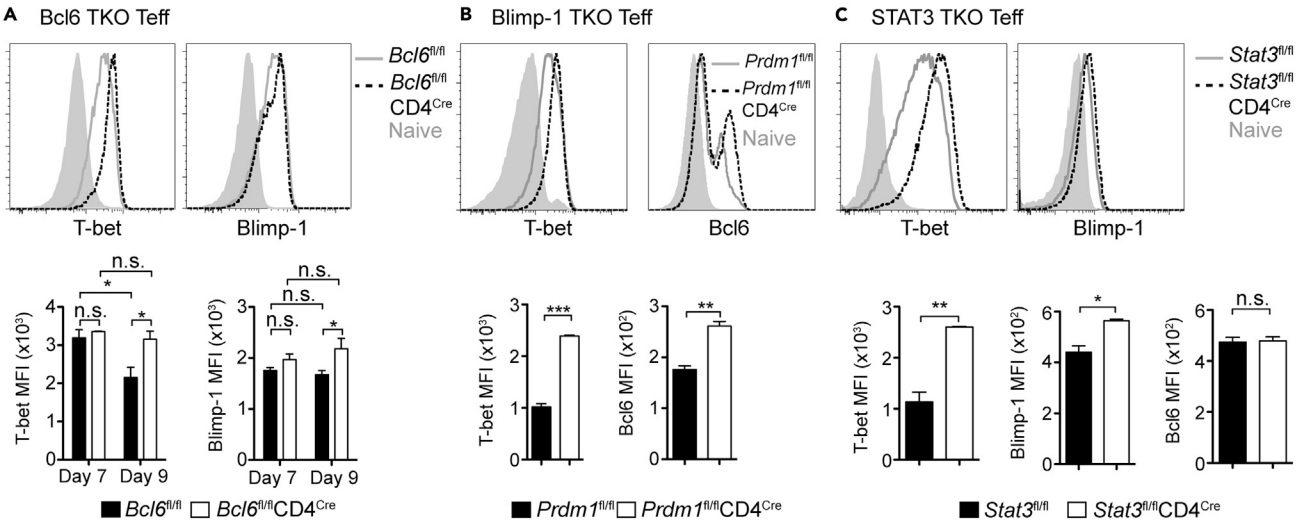

Figure 6. Bcl6, Blimp-1, and STAT3 Control T-bet Expression during *P. chabaudi* Infection

TKO and WT animals were infected and splenocytes were analyzed.

(A) Expression of T-bet (left) and Blimp-1 (right) in Teff from Bcl6 TKO (*Bcl6*$^{fl/fl}$CD4^{Cre}, dotted line), WT (*Bcl6*$^{fl/fl}$, gray line), and naive (gray filled line) cells at day 9 p.i. Bar graphs show average MFI of T-bet and Blimp-1 at days 7 and 9 p.i.

(B) Expression of T-bet (left) and Bcl6 (right) in Teff from Blimp-1 TKO (*Prdm1*$^{fl/fl}$CD4^{Cre}, dotted line) and WT (*Prdm1*$^{fl/fl}$, gray line) animals and naive (gray filled line) cells at day 7 p.i. Bar graphs show average MFI of T-bet and Bcl6 at day 7 p.i.

(C) Expression of T-bet (left) and Blimp-1 (right) expression in Teff from STAT3 TKO (*Stat3*$^{fl/fl}$CD4^{Cre}, dotted line) and WT (*Stat3*$^{fl/fl}$, gray line) animals and naive (gray filled line) cells at day 7 p.i. Bar graphs show average MFI of T-bet, Blimp-1, and Bcl6 expression.

Data representative of 3 experiments with 3–4 mice/group. Data are represented as mean ± SEM. * p <0.05, ** p <0.01, *** p <0.001, **** p >0.05, n.s, not significant. See also Figure S7.

The increase in Th1-like (IFN-γ^{+}IL-21^{-}) cells, decrease in *Plasmodium*-specific serum antibody, and concomitant very strong protection in STAT3 TKO mice support a role for Th1 cells rather than antibody in reinfection. Therefore, we tested the importance of Th1 cells in immunity by giving T-bet KO mice a second infection (Figure 8). T-bet KO mice showed prolonged parasite growth compared with WT mice, with days 6 and 7 p.r.i. remaining uncontrolled (Figure 8A). This was the opposite phenotype to STAT3 TKO, as predicted. Upon *P. chabaudi* reinfection, Teff in T-bet-deficient mice still produced IL-21, but little IFN-γ (Figure 8B). T-bet-deficient mice had increased levels of *P. chabaudi*-specific IgG, but lower levels of Th1-isotype IgG2b (Figure 8C). Furthermore, we observed a significant increase in the proportions of GC Tfh cells that could explain the aberrant isotype switching (Figure 8D). In summary, T cell-intrinsic STAT3 regulates the Th1 bias of memory T cells in *P. chabaudi* infection. Importantly, Th1 cells promote immunity, in addition to the role of pre-existing antibody, particularly IgG2b (Su and Stevenson, 2002).

DISCUSSION

Both Th1 and Tfh cells are required to eliminate parasites in *Plasmodium* infection. Previous work on the immune response to *P. chabaudi* shows that IFN-γ controls the height of the peak of parasitemia, whereas Tfh and IL-21 are required for antibodies to eliminate the parasite (Perez-Mazliah et al., 2015, 2017; Su and Stevenson, 2002; Gbedande et al., 2020; Meding and Langhorne, 1991). We have found that both types of effector functions are combined in one cell type in this infection (Carpio et al., 2015). Although there are certainly GC Tfh that make IFN-γ, we continue to term the multi-functional Teff cells found in persistent infections hybrid Th1/Tfh, rather than Th1-like Tfh, due to the larger effect and active regulation of T-bet (which controls their IFN-γ production) and the smaller effect of Bcl6 (suggesting a more Th1-like lineage), as well as their lack of the true GC Tfh (CXCR5^{hi}PD-1^{hi}) phenotype. It is important to note that in some staining combinations, two populations (i.e., CXCR5^{int}T-bet^{hi}, CXCR5^{lo}T-bet^{int}) appeared detectable within the hybrid population by fluorescence-activated cell sorting, as previously predicted by single cell RNA sequencing analysis (Lonnberg et al., 2017). While the populations are separable, as now clearly shown by CXCR6 staining of the Th1-like population (Soon MSF, et al, 2019), we would argue that the CXCR5^{int} population we detect here, and the two plastic populations within it, do not represent truly differentiated populations, but rather two ends of a continuum. However, we agree that this population can intuitively be

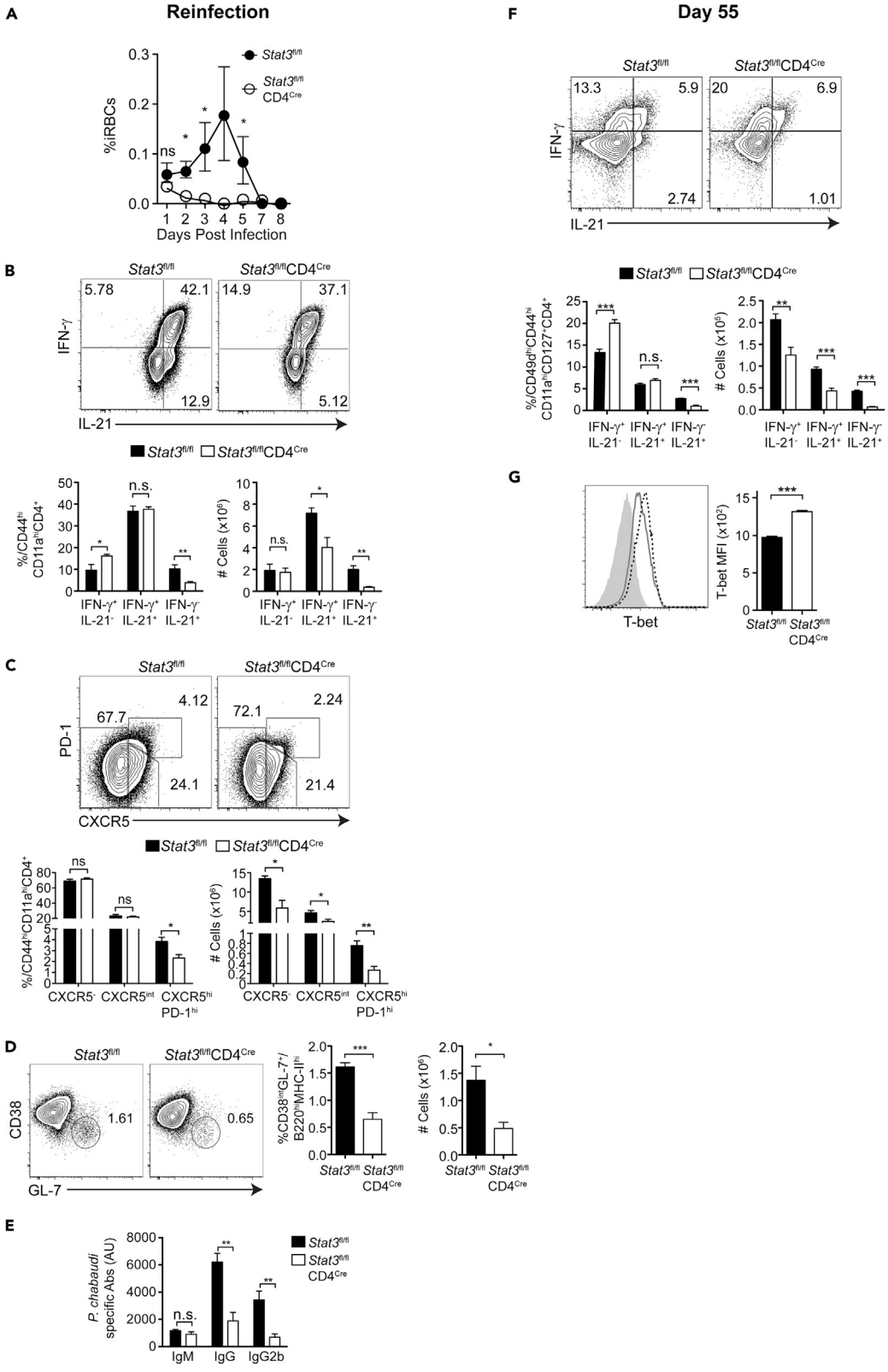
A
Reinfection
%iRBCs
Days Post Infection
Stat3fl/fl
Stat3fl/fl CD4Cre
B
IFN-γ
IL-21
5.78
42.1
12.9
14.9
37.1
5.12
%/CD44hi CD11ahi CD4+
Cells (x10⁶)
IFN-γ+ IL-21-
IFN-γ+ IL-21+
IFN-γ- IL-21+
n.s.
C
PD-1
CXCR5
67.7
4.12
24.1
72.1
2.24
21.4
%/CD44hi CD11ahi CD4+
CXCR5- PD-1hi
CXCR5int PD-1hi
CXCR5hi PD-1hi
D
CD38
GL-7
1.61
0.65
%CD38intGL-7+/ B220intMHC-IIhi
E
P. chabaudi specific Abs (AU)
IgM
IgG
IgG2b
F
Day 55
IFN-γ
IL-21
13.3
5.9
2.74
20
6.9
1.01
%/CD49dhi CD44hi CD11ahi CD127- CD4+
G
T-bet
T-bet MFI (x10³)

Figure 7. STAT3 TKO Mice Are Protected from Reinfection Despite Weaker Humoral Response

STAT3 TKO (*Stat3*$^{fl/fl}$CD4^{Cre}) and WT (*Stat3*$^{fl/fl}$) animals were infected. At day 60 p.i. both groups were treated with chloroquine (CQ) before reinfection at 6 weeks with 10^7 iRBCs.

(A) Parasitemia of WT (filled circles) and STAT3 TKO (open circles) animals.

(B and C) Expression of (B) IFN-γ and IL-21 and (C) PD-1 and CXCR5 by antigen-experienced CD4 T cells (CD44^{hi}CD11a^{hi}) from STAT3 TKO and WT animals at day 7 post-re-infection. Bar graphs show percentages and numbers.

(D) Expression of CD38 and GL-7 in B cells (B220$^+$MHCII$^+$) at day 7 post-re-infection. Bar graphs show percentages and numbers.

(E) Bar graphs showing *P. chabaudi*-specific IgM, IgG, and IgG2b at day 7 post-re-infection.

(F) Expression of IFN-γ and IL-21 in Tmem (CD44^{hi}CD11a^{hi}CD49d^{hi}) from STAT3 TKO and WT animals at day 55 p.i. (first infection). Bar graphs show percentages and numbers.

(G) Expression of T-bet in Tmem from WT (gray line) and STAT3 TKO (dotted black line) animals and naive (gray filled line) cells at day 55 p.i. Bar graph shows MFI of T-bet.

Data representative of 2 experiments, 4–5 mice/group. Data in (A) are pooled from 2 independent experiments, 3–5 mice/group/experiment. Data are represented as mean ± SEM. * p <0.05, ** p <0.01, *** p <0.001, **** p >0.05, n.s, not significant.

termed more Th1- or Tfh-like, as has been the convention in the literature to date. The fact that each feature of these cells is actively regulated by so many transcription factors highlights their plasticity, as a necessity of adapting to the current infection-mediated cytokine milieu. Therefore, we conclude that the Teff population in this infection is not made up of subsets, but is a plastic, heterogeneous, hybrid population that is actively regulated by multiple inputs and transcription factors throughout the infection.

Protection from repeated episodes of malaria in humans correlates with serum IFN-γ and memory Th1 cells (Luty et al., 1999; Moormann et al., 2013; Stephens and Langhorne, 2010). CD4 T cells in adults from malaria-endemic areas also express cytokines of multiple lineages including IFN-γ, IL-10, and IL-21, even in cells with a Tfh-like phenotype (Obeng-Adjei et al., 2015; Roetynck et al., 2013). Human Teff expressing both CXCR3 and CXCR5 and mouse CXCR5$^+$ Teff expressing markers of a high level of activation (Ly6C, NK1.1) can help B cells make antibody; however, they are less effective helper cells *in vitro* than those expressing only CXCR5 (Obeng-Adjei et al., 2015; Zander et al., 2017; Wikenheiser et al., 2018). In humans, CXCR3$^+$CXCR5$^+$ T cells were not shown to correlate with *Plasmodium*-specific antibody levels (Obeng-Adjei et al., 2015). Strikingly, hybrid Th1/Tfh cells (ICOS$^+$CXCR3$^+$CXCR5$^+$) did correlate with antibody levels in influenza, where they were also shown to contain IFN-γ$^+$IL-21$^+$ T cells (Bentebibel et al., 2013). Acute infections, like those caused by *Listeria*, can induce a stable Th1 memory phenotype (Curtis et al., 2010; Hale et al., 2013), whereas chronic LCMV and tuberculosis infections have T cell responses skewed away from a committed Th1 phenotype, and toward concomitant expression of Tfh markers in mice (Crawford et al., 2014; Li et al., 2016). Therefore, Th phenotype plasticity appears to be a shared feature of the immune response to persistent infections and has been shown to be beneficial in control of tuberculosis (Khader et al., 2007; O'Shea and Paul, 2010). Similarly, our data suggest that preserving plasticity would be optimal for protection.

We found that T-bet regulates cytokine production in T cells in *P. chabaudi* infection. In addition, the expression of T-bet is highly regulated, including by STAT3, Blimp-1, and Bcl6, presumably to avoid immunopathology. T-bet expression kinetics also support ongoing regulation. We previously observed that T-bet is downregulated before day 9, the peak of *Ifng*$^+$ T cell expansion (Carpio et al., 2015). Here, we show that this downregulation occurs in a Bcl6-dependent manner. Although T-bet is generally induced by STAT1 in CD4 T cells (Afkarian et al., 2002), and upregulated upon IL-12 signaling through STAT4, neither STAT4 nor STAT1 deficiency negatively regulated the hybrid cytokine profile in T cells. This observation suggests that T-bet in this infection is induced primarily by TCR signaling and IL-18 and/or that there is some redundancy between STATs. T-bet regulation is a critical focus in the control of Th plasticity in this persistent infection.

The hybrid T cell dominant at the peak of infection facilitates strong early cellular and humoral responses. However, the two types of responses clearly also regulate one another. T-bet in T cells has recently been shown to impair GC Tfh cell differentiation and GC formation (Ryg-Cornejo et al., 2016), though it is critical in B cells (Ly et al., 2019). On the other hand, a recent study concluded that T-bet and STAT4 are actually required for GC Tfh development and GC formation during acute viral infection (Weinstein et al., 2018). We confirm that STAT4 is also required for GC Tfh in *P. chabaudi* infection. We did not detect any change in the number of GC Tfh in T-bet-deficient animals infected with *P. chabaudi* during the primary infection as seen in *Plasmodium berghei* ANKA. However, we observed a significant reduction in the percentage of GC Tfh in the secondary infection in T-bet KO mice. T-bet, presumably in its capacity for driving IFN-γ in T cells and thereby promoting production of the IgG2 isotype of antibody, was essential for full parasite control in both the first and second infections. Clearly, the regulation of T-bet and IFN-γ is a high priority for promoting an effective Teff response and survival

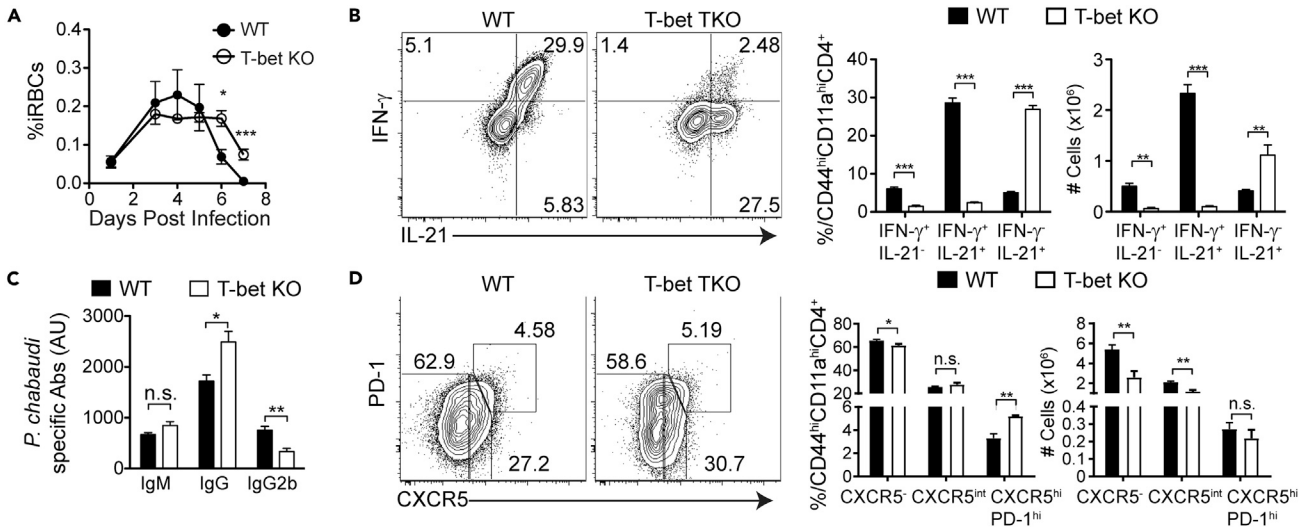

Figure 8. T-bet KO Mice Have Few Th1 Memory Cells, Reduced IgG2b, and Prolonged Parasitemia on Reinfection

(A, B, and D) T-bet KO and WT animals were infected. At day 60 p.i. both groups were treated with chloroquine (CQ) before reinfection. After 3 weeks mice were re-infected with 10^7 iRBCs. (A) Parasitemia of WT (filled circles) and T-bet KO (open circles) animals. Expression of (B) IFN-γ and IL-21 and (D) PD-1 and CXCR5 by antigen-experienced CD4 T cells ($CD44^{hi}CD11a^{hi}$) from T-bet KO and WT animals at day 7 post-reinfection. Bar graphs show percentages and numbers.
(C) Bar graphs showing *P. chabaudi*-specific IgM, IgG, and IgG2b at day 7 post-re-infection.
Data representative of 1 experiment, 3–5 mice/group. Data are represented as mean ± SEM. * p <0.05, ** p <0.01, *** p <0.001, **** p >0.05, n.s, not significant.

of the animals given the multiple transcription factors involved. However, the production of different cytokines during continued infection leads to functional T cell plasticity due to the unique regulation of functional attribute, and overlap in TCR, co-stimulation, and cytokine signaling cascades.

Overlapping signaling cascades control the balance of Th1 and Tfh programs (Weinmann, 2014). IL-12, the primary cytokine responsible for induction of Th1 cells can be essential for generation of Tfh *in vivo* and can also induce IL-10 (Saraiva et al., 2009; Weinstein et al., 2018). In addition, *in vitro*-generated Th1 cells transiently express Bcl6 and IL-21, whereas Tfh transiently express T-bet (Fang et al., 2018; Nakayamada et al., 2011). T-bet can bind and inhibit the Tfh-driving transcription factor, Bcl6 (Oestreich et al., 2012). On the other hand, T cells that express T-bet will not necessarily express IFN-γ, particularly if they also express the transcriptional Bcl6 (Oestreich et al., 2011). Although we previously showed that Bcl6 levels correlate with the level of *Ifng* transcription in intact mice (Carpio et al., 2015), the Bcl6 TKO Teff do not have more IFN-γ protein by intracellular cytokine staining here. Both STAT3 and Bcl6 are reported to be required for Tfh differentiation, whereas Blimp-1 inhibits both Th1 and Tfh differentiation (Cimmino et al., 2008; Johnston et al., 2009; Ma et al., 2012; Nurieva et al., 2009; Ray et al., 2014). However, in our studies, deficiency in either Bcl6 or STAT4 in T cells eliminated GC Tfh, whereas STAT3 deficiency did not. STAT3 deficiency did, however, reduce the proportions of GC Tfh in the setting of a shorter *P. chabaudi* infection, in agreement with previous reports that used acute infections as stimuli (Ray et al., 2014). In addition, we consistently observed that STAT3-deficient T cells did not develop into Tfh-like $IFN\text{-}\gamma^{-}IL\text{-}21^{+}$ Teff in both *P. yoelii* and *P. chabaudi* infections. The shorter infection also resulted in an increase of GC B cells, similar to the increase in GC B cells induced by inactivated *P. berghei* ANKA (Ryg-Cornejo et al., 2016). Given the differences in regulation in shorter versus longer infections shown here, the regulation of *prdm1* expression by type1-I IFN is likely central to the regulation of terminal Tfh differentiation and the increased plasticity during prolonged infection (Zander et al., 2016). Bcl6 also reduced the level of expression of CXCR5, whereas Blimp-1 had the opposite effect. Our data suggest that Bcl6 and Blimp-1 have a stronger effect on regulation of CXCR5 expression than on production of IFN-γ or IL-21. This may be explained by the inhibition by Bcl6 of microRNAs that control *cxcr5* expression (Yu et al., 2009).

The most compelling result here is that skewing the hybrid-lineage cells toward a more committed Th1 phenotype in STAT3 TKO dramatically sped up clearance of parasitemia on reinfection. Supporting this interpretation, T-bet-deficient mice, with less Th1 bias and more $IFN\text{-}\gamma^{-}IL\text{-}21^{+}$ T cells, were significantly

slower at clearing a second infection. While the protection did not correlate with antibody levels, we did not rule out a role for antibody, particularly affinity maturation and isotype switching, in the improved immunity of STAT3 TKO. The mechanism of evolutionary pressure regulating this balance becomes clear in that the shift toward Th1 in STAT3 TKO animals, as well as the shift away from Th1 in the T-bet KO, as also shown for *P. berghei* ANKA, both prolong high parasitemia and pathology in the first infection. STAT3 has been previously suggested to be able to promote Tfh and inhibit Th1 differentiation (Ray et al., 2014; Wu et al., 2015). We found that IL-6 had no impact on the differentiation of Teff. Although IL-27Rα-deficient animals have long been known to have a hyperactive T cell response to pathogens including *Plasmodium*, we have shown that IL-27Rα on T cells regulates the balance between IFN-γ and IL-21 and GC Tfh differentiation, which is supported by the work of others (Batten et al., 2010; Guthmiller et al., 2017; Gwyer Findlay et al., 2014; Hibbert et al., 2003; Kane et al., 2014; Ma et al., 2012; Stumhofer et al., 2007). Supporting our analysis, IL-27 has been shown to be made by CD4 T cells in *Plasmodium* infection (Kimura et al., 2016). It would be of great interest to dissect the molecular pathway that IL-27 uses to guide cytokine production versus its effect on GC Tfh differentiation, for example, the relative role of STAT1 and STAT3 in each. Recent studies have shown that IL-12 can promote STAT3 association with the *bcl6* and *il21* loci in T cells *in vitro*, suggesting a possible signaling pathway for the regulation of plastic Th1 and Tfh populations in the context of complex cytokine milieus (Powell et al., 2019).

Previous studies have demonstrated that the delicate balance of a *P. chabaudi*-infected animal's life or death is regulated by CD4 T cells, as is the case in other persistent infections such as tuberculosis and toxoplasmosis (Caruso et al., 1999; Denkers and Gazzinelli, 1998; Stephens et al., 2005). Animals deficient in either of the pro-Th1 factors IL-12 or IFN-γ, or the regulatory cytokine IL-10, are more susceptible to die of *P. chabaudi* infection, even though it is a normally mild infection in mice (Li et al., 1999; Su and Stevenson, 2000, 2002). T-bet has been shown to be required for control of *P. berghei* ANKA parasitemia but is also essential for pathogenesis of experimental cerebral malaria (Oakley et al., 2013). Although we did not see any mortality from an increase in Th1-type cells in the infected STAT3 TKO, mice that either had more (STAT3) or less (T-bet) IFN-γ^{+}IL-21^{-} Th1-type cells had prolonged pathology. Therefore, although our data, and the human literature, suggest that a stronger Th1 response is beneficial for immunity to *P. chabaudi*, it remains to be tested if the combination of Th1/Tfh and regulatory cytokines into one cell type represents an evolutionary benefit, particularly in the first infection, which is likely to drive evolution the most (next to pregnancy malaria). Further work considering the finely-tuned balance required to ensure host survival is needed to determine if this hybrid response is maladaptive.

In summary, persistent *Plasmodium* infection drives generation of a plastic mixed-lineage T cell with characteristics of both uncommitted Th1 (T-bet^{int}) and pre-Tfh (CXCR5^{int}), that is balanced by STAT3, Bcl6, Blimp-1, and T-bet, which coordinate the relative degree of antibody and IFN-γ responses for optimal pathogen control and host survival. Changing this balance toward Th1 in the first infection may prolong pathology, whereas it promotes sterilizing immunity in the longer term, suggesting a potential direction for vaccine development.

Limitations of the Study

Defining Th1 and Tfh cells by the markers they express can both enhance and limit our understanding. However, we have focused on three markers (CXCR5, IFN-γ, and IL-21) with functional consequences and assays with good discrimination of positive and negative. In addition, most of the Teff population appears to express both T-bet and Bcl6; however, flow cytometry does not report on transcriptional activation. As both Th1/Tfh and GC Tfh express both CXCR5 and CXCR3, it will be important to study the location of each cell type and interactions with B cells *in vivo* in our next study. Although we have used multiple models of rodent malaria, and the predictions from these models are often predictive of human malaria immunology (Stephens et al., 2012; Gbedande et al., 2020), there are likely to be differences of degree in *P. falciparum* infection. These models have the potential to inform other immune environments including other persistent pathogens and the response to transformed cells *in vivo*.

Resource Availability

Lead Contact

Further information and requests for resources and reagents should be directed to, and will be fulfilled by, the Lead Contact, Robin Stephens (rostephe@utmb.edu).

Materials Availability

This study did not generate new unique reagents.

Data and Code Availability

This study did not generate/analyze datasets/code.

METHODS

All methods can be found in the accompanying Transparent Methods supplemental file.

SUPPLEMENTAL INFORMATION

Supplemental Information can be found online at https://doi.org/10.1016/j.isci.2020.101310.

ACKNOWLEDGMENTS

This work was supported by the NIH National Institute of Allergy and Infectious Diseases (R01AI08995304 [R.S., V.H.C.], R01AI135061 [R.S., V.H.C., F.A.], R01AI132771 [A.L.D.], R01AI08995304S1 [R.S., V.H.C.], and F31AI126809 [V.H.C.]) and the James W. McLaughlin and Jeane B. Kempner Fellowships (V.H.C., K.D.W.). We appreciate the expertise of Mark Griffin in the UTMB Microbiology & Immunology Flow Cytometry Core, and Gabriela M. Kaus and Margarita Ramirez for expert animal colony maintenance. We appreciate the scientific contribution of all Stephens and Joint Immunology Lab meeting members (Y. Cong, J. Sun, H. Hu, J.J. Endsley, R. Rajsbaum, L. Soong). Thanks to Roza I. Nurieva, John O'Shea, and Noah S. Butler for ideas, reagents, and protocols.

AUTHOR CONTRIBUTIONS

Conceptualization, V.H.C. and R.S.; Methodology, V.H.C. and R.S.; Investigation, V.H.C., F.A., K.D.W., and F.A.; Writing – Original Draft, V.H.C.; Writing – Review & Editing, V.H.C., L.P.-C., R.S., and A.L.D.; Funding Acquisition, R.S., V.H.C., and A.L.D.; Resources, A.L.D., A.V.V., and R.S.

DECLARATION OF INTERESTS

The authors declare no competing interests.

Received: December 20, 2019
Revised: May 20, 2020
Accepted: June 19, 2020
Published: July 24, 2020

REFERENCES

Afkarian, M., Sedy, J.R., Yang, J., Jacobson, N.G., Cereb, N., Yang, S.Y., Murphy, T.L., and Murphy, K.M. (2002). T-bet is a STAT1-induced regulator of IL-12R expression in naive CD4+ T cells. Nat. Immunol. *3*, 549–557.

Batten, M., Ramamoorthi, N., Kljavin, N.M., Ma, C.S., Cox, J.H., Dengler, H.S., Danilenko, D.M., Caplazi, P., Wong, M., Fulcher, D.A., et al. (2010). IL-27 supports germinal center function by enhancing IL-21 production and the function of T follicular helper cells. J. Exp. Med. *207*, 2895–2906.

Bentebibel, S.E., Lopez, S., Obermoser, G., Schmitt, N., Mueller, C., Harrod, C., Flano, E., Mejias, A., Albrecht, R.A., Blankenship, D., et al. (2013). Induction of ICOS+CXCR3+CXCR5+ TH cells correlates with antibody responses to influenza vaccination. Sci. Transl. Med. *5*, 176ra132.

Carpio, V.H., Opata, M.M., Montanez, M.E., Banerjee, P.P., Dent, A.L., and Stephens, R. (2015). IFN-gamma and IL-21 double producing T cells are Bcl6-independent and survive into the memory phase in *Plasmodium chabaudi* infection. PLoS One *10*, e0144654.

Caruso, A.M., Serbina, N., Klein, E., Triebold, K., Bloom, B.R., and Flynn, J.L. (1999). Mice deficient in CD4 T cells have only transiently diminished levels of IFN-gamma, yet succumb to tuberculosis. J. Immunol. *162*, 5407–5416.

Choi, Y.S., Eto, D., Yang, J.A., Lao, C., and Crotty, S. (2013). Cutting edge: STAT1 is required for IL-6-mediated Bcl6 induction for early follicular helper cell differentiation. J. Immunol. *190*, 3049–3053.

Cimmino, L., Martins, G.A., Liao, J., Magnusdottir, E., Grunig, G., Perez, R.K., and Calame, K.L. (2008). Blimp-1 attenuates Th1 differentiation by repression of *ifng*, *tbx21*, and *bcl6* gene expression. J. Immunol. *181*, 2338–2347.

Crawford, A., Angelosanto, J.M., Kao, C., Doering, T.A., Odorizzi, P.M., Barnett, B.E., and Wherry, E.J. (2014). Molecular and transcriptional basis of CD4(+) T cell dysfunction during chronic infection. Immunity *40*, 289–302.

Crotty, S. (2014). T follicular helper cell differentiation, function, and roles in disease. Immunity *41*, 529–542.

Curtis, M.M., Rowell, E., Shafiani, S., Negash, A., Urdahl, K.B., Wilson, C.B., and Way, S.S. (2010). Fidelity of pathogen-specific CD4+ T cells to the Th1 lineage is controlled by exogenous cytokines, interferon-gamma expression, and pathogen lifestyle. Cell Host Microbe *8*, 163–173.

Denkers, E.Y., and Gazzinelli, R.T. (1998). Regulation and function of T-cell-mediated immunity during *Toxoplasma gondii* infection. Clin. Microbiol. Rev. *11*, 569–588.

Elsaesser, H., Sauer, K., and Brooks, D.G. (2009). IL-21 is required to control chronic viral infection. Science *324*, 1569–1572.

Fahey, L.M., Wilson, E.B., Elsaesser, H., Fistonich, C.D., McGavern, D.B., and Brooks, D.G. (2011). Viral persistence redirects CD4 T cell differentiation toward T follicular helper cells. J. Exp. Med. *208*, 987–999.

Fang, D., Cui, K., Mao, K., Hu, G., Li, R., Zheng, M., Riteau, N., Reiner, S.L., Sher, A., Zhao, K., et al. (2018). Transient T-bet expression functionally specifies a distinct T follicular helper subset. J. Exp. Med. *215*, 2705–2714.

Freitas do Rosario, A.P., Lamb, T., Spence, P., Stephens, R., Lang, A., Roers, A., Muller, W., O'Garra, A., and Langhorne, J. (2012). IL-27 promotes IL-10 production by effector Th1 CD4+ T cells: a critical mechanism for protection from severe immunopathology during malaria infection. J. Immunol. *188*, 1178–1190.

Gbedande, K., Carpio, V.H., and Stephens, R. (2020). Using two phases of the CD 4 T cell response to blood-stage murine malaria to understand regulation of systemic immunity and placental pathology in *Plasmodium falciparum* infection. Immunol. Rev. *293*, 88–114.

Guthmiller, J.J., Graham, A.C., Zander, R.A., Pope, R.L., and Butler, N.S. (2017). Cutting edge: IL-10 is essential for the generation of germinal center B cell responses and anti-*Plasmodium* humoral immunity. J. Immunol. *198*, 617–622.

Gwyer Findlay, E., Villegas-Mendez, A., O'Regan, N., de Souza, J.B., Grady, L.M., Saris, C.J., Riley, E.M., and Couper, K.N. (2014). IL-27 receptor signaling regulates memory CD4+ T cell populations and suppresses rapid inflammatory responses during secondary malaria infection. Infect. Immun. *82*, 10–20.

Hale, J.S., Youngblood, B., Latner, D.R., Mohammed, A.U., Ye, L., Akondy, R.S., Wu, T., Iyer, S.S., and Ahmed, R. (2013). Distinct memory CD4+ T cells with commitment to T follicular helper- and T helper 1-cell lineages are generated after acute viral infection. Immunity *38*, 805–817.

Hibbert, L., Pflanz, S., De Waal Malefyt, R., and Kastelein, R.A. (2003). IL-27 and IFN-alpha signal via *Stat1* and *Stat3* and induce T-Bet and IL-12Rbeta2 in naive T cells. J. Interferon Cytokine Res. *23*, 513–522.

Hsieh, C.S., Macatonia, S.E., Tripp, C.S., Wolf, S.F., O'Garra, A., and Murphy, K.M. (1993). Development of TH1 CD4+ T cells through IL-12 produced by Listeria-induced macrophages. Science *260*, 547–549.

Hunt, P., Cravo, P.V., Donleavy, P., Carlton, J.M., and Walliker, D. (2004). Chloroquine resistance in *Plasmodium chabaudi*: are chloroquine-resistance transporter (crt) and multi-drug resistance (mdr1) orthologues involved? Mol. Biochem. Parasitol. *133*, 27–35.

Johnston, R.J., Poholek, A.C., DiToro, D., Yusuf, I., Eto, D., Barnett, B., Dent, A.L., Craft, J., and Crotty, S. (2009). Bcl6 and Blimp-1 are reciprocal and antagonistic regulators of T follicular helper cell differentiation. Science *325*, 1006–1010.

Kane, A., Deenick, E.K., Ma, C.S., Cook, M.C., Uzel, G., and Tangye, S.G. (2014). STAT3 is a central regulator of lymphocyte differentiation and function. Curr. Opin. Immunol. *28*, 49–57.

Khader, S.A., Bell, G.K., Pearl, J.E., Fountain, J.J., Rangel-Moreno, J., Cilley, G.E., Shen, F., Eaton, S.M., Gaffen, S.L., Swain, S.L., et al. (2007). IL-23 and IL-17 in the establishment of protective pulmonary CD4+ T cell responses after vaccination and during *Mycobacterium tuberculosis* challenge. Nat. Immunol. *8*, 369–377.

Kimura, D., Miyakoda, M., Kimura, K., Honma, K., Hara, H., Yoshida, H., and Yui, K. (2016). Interleukin-27-producing CD4(+) T cells regulate protective immunity during malaria parasite infection. Immunity *44*, 672–682.

Li, C., Corraliza, I., and Langhorne, J. (1999). A defect in interleukin-10 leads to enhanced malarial disease in *Plasmodium chabaudi chabaudi* infection in mice. Infect. Immun. *67*, 4435–4442.

Li, C., Sanni, L.A., Omer, F., Riley, E., and Langhorne, J. (2003). Pathology of *Plasmodium chabaudi chabaudi* infection and mortality in interleukin-10-deficient mice are ameliorated by anti-tumor necrosis factor alpha and exacerbated by anti-transforming growth factor beta antibodies. Infect. Immun. *71*, 4850–4856.

Li, L., Jiang, Y., Lao, S., Yang, B., Yu, S., Zhang, Y., and Wu, C. (2016). *Mycobacterium tuberculosis*-specific IL-21+IFN-gamma+CD4+ T cells are regulated by IL-12. PLoS One *11*, e0147356.

Lonnberg, T., Svensson, V., James, K.R., Fernandez-Ruiz, D., Sebina, I., Montandon, R., Soon, M.S., Fogg, L.G., Nair, A.S., Liligeto, U., et al. (2017). Single-cell RNA-seq and computational analysis using temporal mixture modelling resolves Th1/Tfh fate bifurcation in malaria. Sci. Immunol. *2*, eaal2192.

Luty, A.J., Lell, B., Schmidt-Ott, R., Lehman, L.G., Luckner, D., Greve, B., Matousek, P., Herbich, K., Schmid, D., Migot-Nabias, F., et al. (1999). Interferon-gamma responses are associated with resistance to reinfection with *Plasmodium falciparum* in young African children. J. Infect. Dis. *179*, 980–988.

Ly, A., Liao, Y., Pietrzak, H., Ioannidis, L.J., Sidwell, T., Gloury, R., Doerflinger, M., Triglia, T., Qin, R.Z., Groom, J.R., et al. (2019). Transcription Factor T-bet in B Cells Modulates Germinal Center Polarization and Antibody Affinity Maturation in Response to Malaria. Cell Rep. *29*, 2257–2269.e6.

Ma, C.S., Avery, D.T., Chan, A., Batten, M., Bustamante, J., Boisson-Dupuis, S., Arkwright, P.D., Kreins, A.Y., Averbuch, D., Engelhard, D., et al. (2012). Functional STAT3 deficiency compromises the generation of human T follicular helper cells. Blood *119*, 3997–4008.

May, J., Lell, B., Luty, A.J., Meyer, C.G., and Kremsner, P.G. (2000). Plasma interleukin-10:Tumor necrosis factor (TNF)-alpha ratio is associated with TNF promoter variants and predicts malarial complications. J. Infect. Dis. *182*, 1570–1573.

McDermott, D.S., and Varga, S.M. (2011). Quantifying antigen-specific CD4 T cells during a viral infection: CD4 T cell responses are larger than we think. J. Immunol. *187*, 5568–5576.

Meding, S., J., and Langhorne, J. (1991). $CD4^+$ T cells and B cells are necessary for the transfer of protective immunity to *Plasmodium chabaudi chabaudi*. Eur. J. Immunol. *21*, 1433–1438.

Montes de Oca, M., Kumar, R., de Labastida Rivera, F., Amante, F.H., Sheel, M., Faleiro, R.J., Bunn, P.T., Best, S.E., Beattie, L., Ng, S.S., et al. (2016). Blimp-1-dependent IL-10 production by Tr1 cells regulates TNF-mediated tissue pathology. PLoS Pathog. *12*, e1005398.

Moormann, A.M., Sumba, P.O., Chelimo, K., Fang, H., Tisch, D.J., Dent, A.E., John, C.C., Long, C.A., Vulule, J., and Kazura, J.W. (2013). Humoral and cellular immunity to *Plasmodium falciparum* merozoite surface protein 1 and protection from infection with blood-stage parasites. J. Infect. Dis. *208*, 149–158.

Nakayamada, S., Kanno, Y., Takahashi, H., Jankovic, D., Lu, K.T., Johnson, T.A., Sun, H.W., Vahedi, G., Hakim, O., Handon, R., et al. (2011). Early Th1 cell differentiation is marked by a Tfh cell-like transition. Immunity *35*, 919–931.

Nurieva, R.I., Chung, Y., Hwang, D., Yang, X.O., Kang, H.S., Ma, L., Wang, Y.H., Watowich, S.S., Jetten, A.M., Tian, Q., et al. (2008). Generation of T follicular helper cells is mediated by interleukin-21 but independent of T helper 1, 2, or 17 cell lineages. Immunity *29*, 138–149.

Nurieva, R.I., Chung, Y., Martinez, G.J., Yang, X.O., Tanaka, S., Matskevitch, T.D., Wang, Y.H., and Dong, C. (2009). Bcl6 mediates the development of T follicular helper cells. Science *325*, 1001–1005.

O'Shea, J.J., and Paul, W.E. (2010). Mechanisms underlying lineage commitment and plasticity of helper CD4+ T cells. Science *327*, 1098–1102.

Oakley, M.S., Sahu, B.R., Lotspeich-Cole, L., Solanki, N.R., Majam, V., Pham, P.T., Banerjee, R., Kozakai, Y., Derrick, S.C., Kumar, S., et al. (2013). The transcription factor T-bet regulates parasitemia and promotes pathogenesis during *Plasmodium berghei* ANKA murine malaria. J. Immunol. *191*, 4699–4708.

Obeng-Adjei, N., Portugal, S., Tran, T.M., Yazew, T.B., Skinner, J., Li, S., Jain, A., Felgner, P.L., Doumbo, O.K., Kayentao, K., et al. (2015). Circulating Th1-cell-type Tfh cells that exhibit impaired B cell help are preferentially activated during acute malaria in children. Cell Rep. *13*, 425–439.

Oestreich, K.J., Huang, A.C., and Weinmann, A.S. (2011). The lineage-defining factors T-bet and Bcl-6 collaborate to regulate Th1 gene expression patterns. J. Exp. Med. *208*, 1001–1013.

Oestreich, K.J., Mohn, S.E., and Weinmann, A.S. (2012). Molecular mechanisms that control the expression and activity of Bcl-6 in TH1 cells to regulate flexibility with a TFH-like gene profile. Nat. Immunol. *13*, 405–411.

Opata, M.M., Carpio, V.H., Ibitokou, S.A., Dillon, B.E., Obiero, J.M., and Stephens, R. (2015). Early effector cells survive the contraction phase in malaria infection and generate both central and effector memory T cells. J. Immunol. *194*, 5346–5354.

Paivandy, A., Calounova, G., Zarnegar, B., Ohrvik, H., Melo, F.R., and Pejler, G. (2014). Mefloquine, an anti-malaria agent, causes reactive oxygen species-dependent cell death in mast cells via a secretory granule-mediated pathway. Pharmacol. Res. Perspect. *2*, e00066.

Parish, I.A., Marshall, H.D., Staron, M.M., Lang, P.A., Brustle, A., Chen, J.H., Cui, W., Tsui, Y.C., Perry, C., Laidlaw, B.J., et al. (2014). Chronic viral infection promotes sustained Th1-derived immunoregulatory IL-10 via BLIMP-1. J. Clin. Invest. *124*, 3455–3468.

Pepper, M., Pagan, A.J., Igyarto, B.Z., Taylor, J.J., and Jenkins, M.K. (2011). Opposing signals from the Bcl6 transcription factor and the interleukin-2 receptor generate T helper 1 central and effector memory cells. Immunity *35*, 583–595.

Perez-Mazliah, D., Ng, D.H., Freitas do Rosario, A.P., McLaughlin, S., Mastelic-Gavillet, B., Sodenkamp, J., Kushinga, G., and Langhorne, J. (2015). Disruption of IL-21 signaling affects T cell-B cell interactions and abrogates protective humoral immunity to malaria. PLoS Pathog. *11*, e1004715.

Perez-Mazliah, D., Nguyen, M.P., Hosking, C., McLaughlin, S., Lewis, M.D., Tumwine, I., Levy, P., and Langhorne, J. (2017). Follicular helper T cells are essential for the elimination of *Plasmodium* infection. EBioMedicine *24*, 216–230.

Powell, M.D., Read, K.A., Sreekumar, B.K., Jones, D.M., and Oestreich, K.J. (2019). IL-12 signaling drives the differentiation and function of a TH1-derived TFH1-like cell population. Sci. Rep. *9*, 13991.

Ray, J.P., Marshall, H.D., Laidlaw, B.J., Staron, M.M., Kaech, S.M., and Craft, J. (2014). Transcription factor STAT3 and type I interferons are corepressive insulators for differentiation of follicular helper and T helper 1 cells. Immunity *40*, 367–377.

Roetynck, S., Olotu, A., Simam, J., Marsh, K., Stockinger, B., Urban, B., and Langhorne, J. (2013). Phenotypic and functional profiling of CD4 T cell compartment in distinct populations of healthy adults with different antigenic exposure. PLoS One *8*, e55195.

Ryg-Cornejo, V., Ioannidis, L.J., Ly, A., Chiu, C.Y., Tellier, J., Hill, D.L., Preston, S.P., Pellegrini, M., Yu, D., Nutt, S.L., et al. (2016). Severe malaria infections impair germinal center responses by inhibiting T follicular helper cell differentiation. Cell Rep. *14*, 68–81.

Saraiva, M., Christensen, J.R., Veldhoen, M., Murphy, T.L., Murphy, K.M., and O'Garra, A. (2009). Interleukin-10 production by Th1 cells requires interleukin-12-induced STAT4 transcription factor and ERK MAP kinase activation by high antigen dose. Immunity *31*, 209–219.

Schulz, E.G., Mariani, L., Radbruch, A., and Hofer, T. (2009). Sequential polarization and imprinting of type 1 T helper lymphocytes by interferon-gamma and interleukin-12. Immunity *30*, 673–683.

Sebina, I., Fogg, L.G., James, K.R., Soon, M.S.F., Akter, J., Thomas, B.S., Hill, G.R., Engwerda, C.R., and Haque, A. (2017). IL-6 promotes CD4(+) T-cell and B-cell activation during *Plasmodium* infection. Parasite Immunol. *39*, e12455.

Sponaas, A.M., Belyaev, N., Falck-Hansen, M., Potocnik, A., and Langhorne, J. (2012). Transient deficiency of dendritic cells results in lack of a merozoite surface protein 1-specific CD4 T cell response during peak *Plasmodium chabaudi* blood-stage infection. Infect. Immun. *80*, 4248–4256.

Stephens, R., Albano, F.R., Quin, S., Pascal, B.J., Harrison, V., Stockinger, B., Kioussis, D., Weltzien, H.U., and Langhorne, J. (2005). Malaria-specific transgenic CD4(+) T cells protect immunodeficient mice from lethal infection and demonstrate requirement for a protective threshold of antibody production for parasite clearance. Blood *106*, 1676–1684.

Stephens, R., Culleton, R.L., and Lamb, T.J. (2012). The contribution of *Plasmodium chabaudi* to our understanding of malaria. Trends Parasitol. *28*, 73–82.

Stephens, R., and Langhorne, J. (2010). Effector memory Th1 CD4 T cells are maintained in a mouse model of chronic malaria. PLoS Pathog. *6*, e1001208.

Stumhofer, J.S., Silver, J.S., Laurence, A., Porrett, P.M., Harris, T.H., Turka, L.A., Ernst, M., Saris, C.J., O'Shea, J.J., and Hunter, C.A. (2007). Interleukins 27 and 6 induce STAT3-mediated T cell production of interleukin 10. Nat. Immunol. *8*, 1363–1371.

Su, Z., and Stevenson, M.M. (2000). Central role of endogenous gamma interferon in protective immunity against blood-stage *Plasmodium chabaudi* AS infection. Infect Immun. *68*, 4399–4406.

Su, Z., and Stevenson, M.M. (2002). IL-12 is required for antibody-mediated protective immunity against blood-stage *Plasmodium chabaudi* AS malaria infection in mice. J. Immunol. *168*, 1348–1355.

Szabo, S.J., Kim, S.T., Costa, G.L., Zhang, X., Fathman, C.G., and Glimcher, L.H. (2000). A novel transcription factor, T-bet, directs Th1 lineage commitment. Cell *100*, 655–669.

Taylor, J.J., Pape, K.A., and Jenkins, M.K. (2012). A germinal center-independent pathway generates unswitched memory B cells early in the primary response. J. Exp. Med. *209*, 597–606.

Tubo, N.J., and Jenkins, M.K. (2014). TCR signal quantity and quality in CD4+ T cell differentiation. Trends Immunol. *35*, 591–596.

Tubo, N.J., Pagan, A.J., Taylor, J.J., Nelson, R.W., Linehan, J.L., Ertelt, J.M., Huseby, E.S., Way, S.S., and Jenkins, M.K. (2013). Single naive CD4+ T cells from a diverse repertoire produce different effector cell types during infection. Cell *153*, 785–796.

Weinmann, A.S. (2014). Regulatory mechanisms that control T-follicular helper and T-helper 1 cell flexibility. Immunol. Cell Biol. *92*, 34–39.

Weinstein, J.S., Laidlaw, B.J., Lu, Y., Wang, J.K., Schulz, V.P., Li, N., Herman, E.I., Kaech, S.M., Gallagher, P.G., and Craft, J. (2018). STAT4 and T-bet control follicular helper T cell development in viral infections. J. Exp. Med. *215*, 337–355.

Wikenheiser, D.J., Ghosh, D., Kennedy, B., and Stumhofer, J.S. (2016). The costimulatory molecule ICOS regulates host Th1 and follicular Th cell differentiation in response to *Plasmodium chabaudi chabaudi* AS infection. J. Immunol. *196*, 778–791.

Wikenheiser, D.J., Brown, S.L., Lee, J., and Stumhofer, J.S. (2018). NK1.1 Expression Defines a Population of CD4 $^{+}$ Effector T Cells Displaying Th1 and Tfh Cell Properties That Support Early Antibody Production During *Plasmodium yoelii* Infection. Front. Immunol. *9*, 2277.

Wu, H., Xu, L.L., Teuscher, P., Liu, H., Kaplan, M.H., and Dent, A.L. (2015). An inhibitory role for the transcription factor Stat3 in controlling IL-4 and Bcl6 expression in follicular helper T cells. J. Immunol. *195*, 2080–2089.

Xu, H., Hodder, A.N., Yan, H., Crewther, P.E., Anders, R.F., and Good, M.F. (2000). CD4+ T cells acting independently of antibody contribute to protective immunity to *Plasmodium chabaudi* infection after apical membrane antigen 1 immunization. J. Immunol. *165*, 389–396.

Yu, D., Rao, S., Tsai, L.M., Lee, S.K., He, Y., Sutcliffe, E.L., Srivastava, M., Linterman, M., Zheng, L., Simpson, N., et al. (2009). The transcriptional repressor Bcl-6 directs T follicular helper cell lineage commitment. Immunity *31*, 457–468.

Zander, R.A., Guthmiller, J.J., Graham, A.C., Pope, R.L., Burke, B.E., Carr, D.J., and Butler, N.S. (2016). Type I interferons induce T regulatory 1 responses and restrict humoral immunity during experimental malaria. PLoS Pathog. *12*, e1005945.

Zander, R.A., Vijay, R., Pack, A.D., Guthmiller, J.J., Graham, A.C., Lindner, S.E., Vaughan, A.M., Kappe, S.H.I., and Butler, N.S. (2017). Th1-like *Plasmodium*-specific memory CD4(+) T cells support humoral immunity. Cell Rep. *21*, 1839–1852.

2. https://www.biorxiv.org/content/10.1101/675967v1. 2019. (Accessed 30 June 2020).

iScience, Volume *23*

Supplemental Information

T Helper Plasticity Is Orchestrated by STAT3, Bcl6, and Blimp-1 Balancing Pathology and Protection in Malaria

Victor H. Carpio, Florentin Aussenac, Lucinda Puebla-Clark, Kyle D. Wilson, Alejandro V. Villarino, Alexander L. Dent, and Robin Stephens

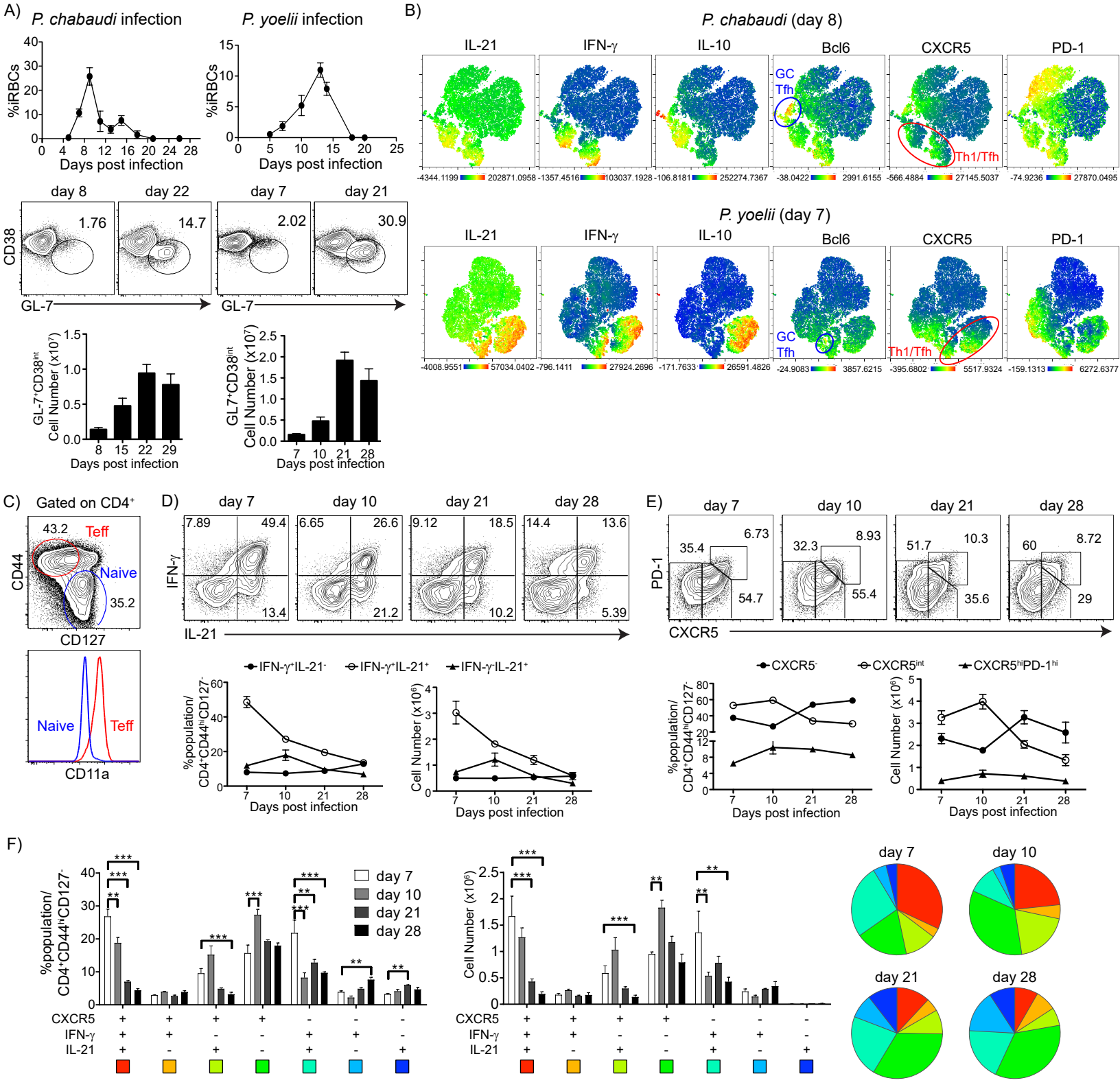

Figure S1. T **helper differentiation during** *P. chabaudi* **and** *P. yoelii* **infections.** *Related to Figure 1.* C57BL/6J mice were infected with either *P. chabaudi* or *P. yoelii* 17XNL and splenocytes analyzed on days indicated. (**A**) Parasitemia, and expression of CD38 and GL-7 in B cells ($B220^+MHCII^+$). Bar graph shows numbers of GC B cells ($CD38^{lo}GL7^+$) at indicated days. (**B**) Density t-SNE plots of $CD4^+$ T cells from C57BL/6J mice infected with *P. chabaudi* at day 8 p.i. or *P. yoelii* at day 7 p.i. Plots show 10^5 representative T cells from each of 3 mice, concatenated and overlaid with the expression of selected markers. (**C**) Expression of CD44, CD127, and CD11a in $CD4^+$ T cells at day 8 of *P. chabaudi* infection showing concordance of $CD127^-$ and $CD11a^{hi}$ as markers of activation. Expression of (**D**) IFN-γ and IL-21 or (**E**) PD-1 and CXCR5 in Teff during *P. yoelii* infection. Line graphs show percentage (left) and numbers (right) of subsets over time. (**F**) Boolean gating of $CXCR5^+$, $IFN\text{-}\gamma^+$, and $IL\text{-}21^+$ of Teff in *P. yoelii* infection at each time point. Pie charts show the distribution of subsets on each day. Bar graphs show the percentages and cell numbers of the subsets on each day. Data representative of 2 experiments with 3 mice/group. Data are represented as mean ± SEM.

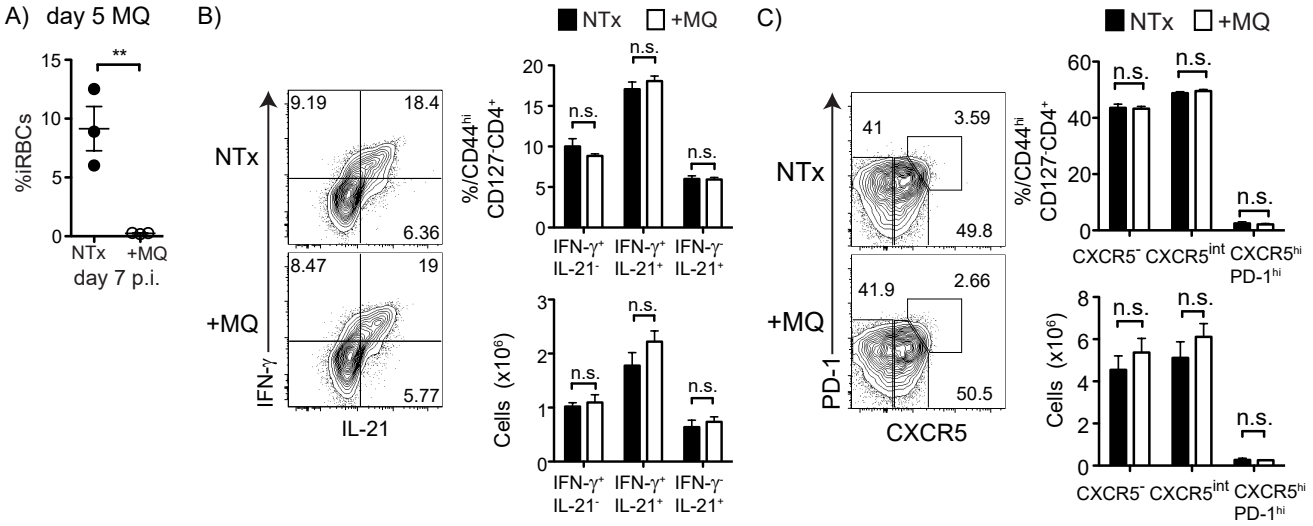

Figure S2. Stopping the infection on day 5 post-infection has no effect on hybrid Th1/Tfh cell phenotype. *Related to Figure 2*. C57BL/6J mice were infected, and one group was treated with mefloquine (MQ) daily starting day 5, and splenocytes were analyzed at day 7 p.i. (**A**) Parasitemia on day 7 p.i. from untreated (NTx, black filled circles) and treated (+MQ, open circles) groups. Expression of (**B**) IFN-γ and IL-21, or (**C**) PD-1 and CXCR5 in Teff. Bar graphs show percentage of Teff (top) and numbers (bottom). Data representative of 2 experiments with 3 mice/group. Data are represented as mean ± SEM.

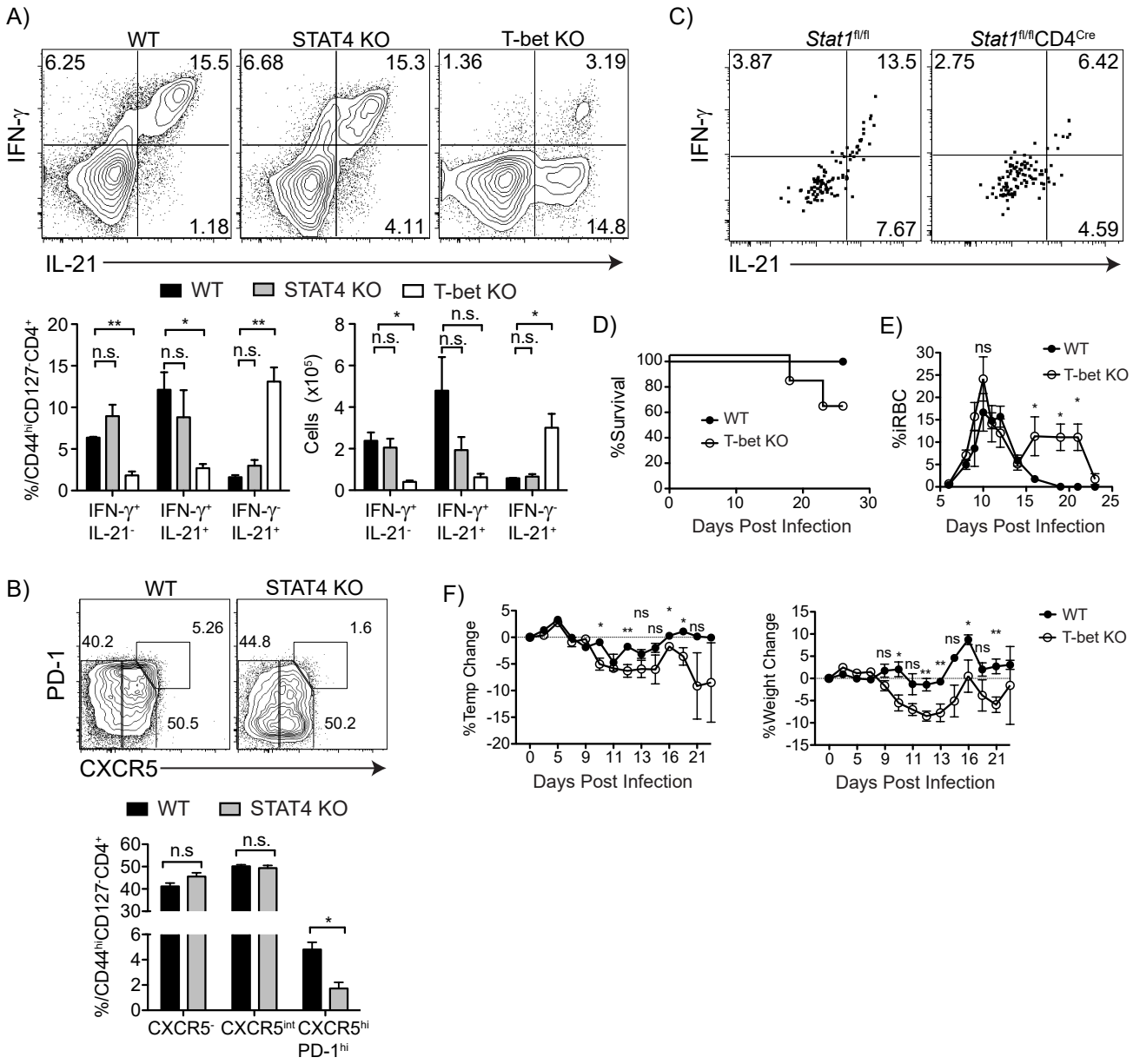

Figure S3. T-bet, but not STAT4 nor STAT1, is required for IFN-γ production by hybrid Th1/Tfh. *Related to Figure 3*. (**A**) C57BL/6J (WT), STAT4 KO, and *Tbx21* (T-bet) KO mice were infected and splenocytes were analyzed at day 7 p.i. Contour plots and bar graphs show expression of IFN-γ and IL-21 in Teff from WT (black bar), STAT4 KO (gray bar) and T-bet KO (white bar). (**B**) Expression of PD-1 and CXCR5 in Teff from WT and STAT4 KO mice at day 7 p.i. Below, bar graphs show percentages. (**C**) Splenocytes from uninfected *Stat1*$^{fl/fl}$CD4^{Cre} (STAT1 TKO) or *Stat1*$^{fl/fl}$ (WT) were labeled with cell trace violet (CTV) and adoptively transferred into Ly5.1 (CD45.1) congenic mice, which were then infected with *P. chabaudi*. Expression of IFN-γ and IL-21 in divided Teff (CTV^{-} gated) on day 8 p.i. (**D**) Survival curve and (**E**) Parasitemia of WT (filled circles) and T-bet KO (open circles) groups. (**F**) Temperature and weight loss of infected WT and T-bet KO groups. Data representative of 2 experiments with 3-8 mice/group for (**A**, **D**, **E**, and **F**) and 1 experiment with 4-5 mice/group for (**C**). Data are represented as mean ± SEM.

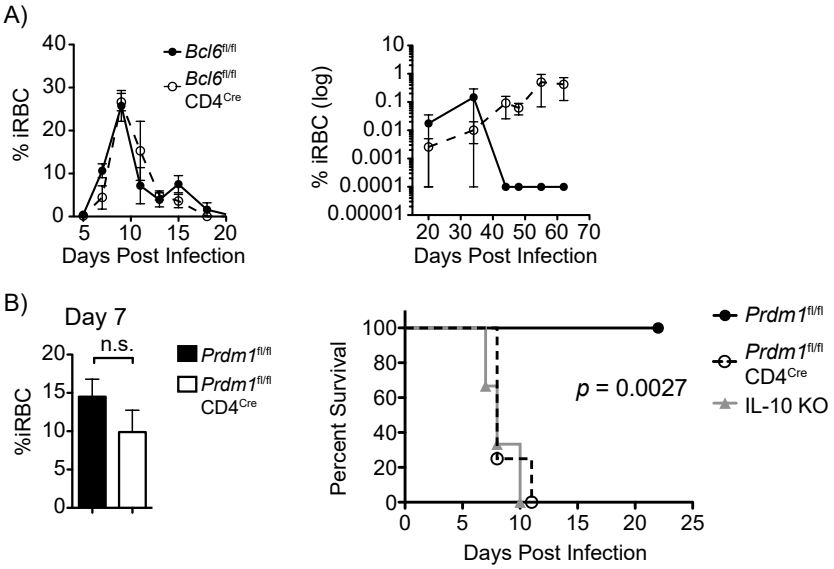

Figure S4. Roles of Bcl6 and Blimp in T cell differentiation during *P. chabaudi* infection. *Related to Figure 4*. (**A**) *Bcl6*$^{fl/fl}$CD4^{Cre} (TKO, open circles) and *Bcl6*$^{fl/fl}$ (WT, filled circles) animals were infected and parasitemia was measured for 2 months. (**B**) *Prdm1*$^{fl/fl}$CD4^{Cre} (Blimp-1 TKO) and *Prdm1*$^{fl/fl}$ (WT) animals were infected and parasitemia was measured at day 7 p.i. Survival of WT (filled circles), Blimp-1 TKO (open circles) and IL-10 KO (gray triangles). Data representative of 3 experiments, 3-4 mice/group. Data are represented as mean ± SEM.

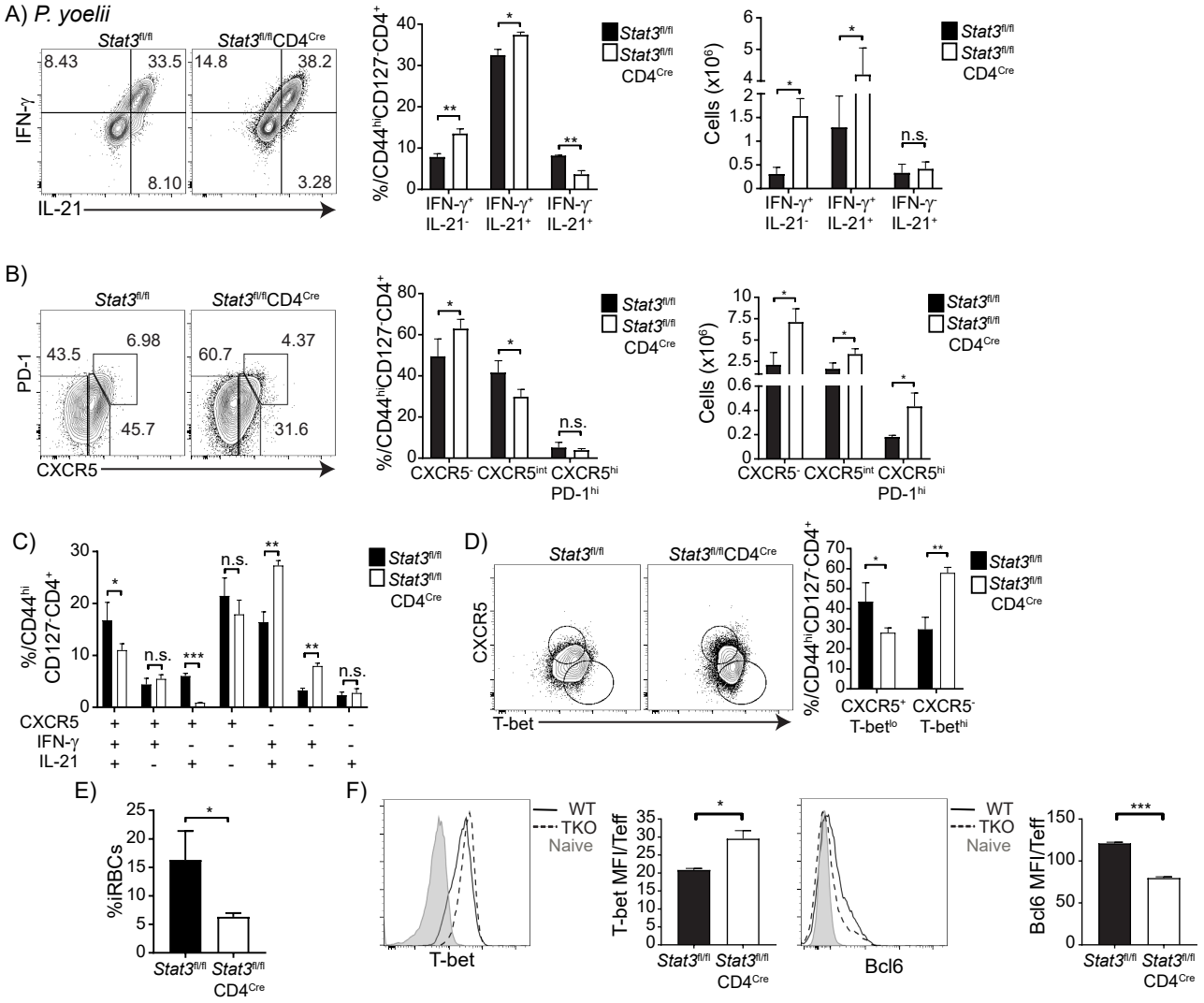

Figure S5. *P. yoelii*-**infected STAT3 TKO mice show similar T cell phenotypes to** *P. chabaudi* **infection.** *Related to Figure 5*. *Stat3*$^{fl/fl}$CD4^{Cre} (TKO) and *Stat3*$^{fl/fl}$ (WT) animals were infected with *P. yoelii* 17XNL and splenocytes were analyzed at day 10 p.i. Expression of (**A**) IFN-γ and IL-21, or (**B**) PD-1 and CXCR5 gated on Teff. Bar graphs show percentages and numbers per spleen. (**C**) Boolean gating of CXCR5^{+}, IFN-γ^{+}, and IL-21^{+} within WT (black bars) and STAT3 TKO (white bars) Teff. (**D**) Contour plots show expression of CXCR5 and T-bet in Teff. Bar graph shows percentages of Tfh-like (CXCR5^{+}T-bet^{lo}) and Th1-like (CXCR5^{-}T-bet^{hi}) Teff. (**E**) Parasitemia of WT (black bars) and STAT3 TKO (white bars) animals on day 10 p.i. (**F**) Histograms showing T-bet (left) and Bcl6 (right) expression in Teff from STAT3 TKO (dotted line) and WT (black line) animals, and naive (gray filled line) cells. Bar graphs shows average MFI of T-bet and Bcl6. Data representative of 1 experiment with 2-3 mice/group. Data are represented as mean ± SEM.

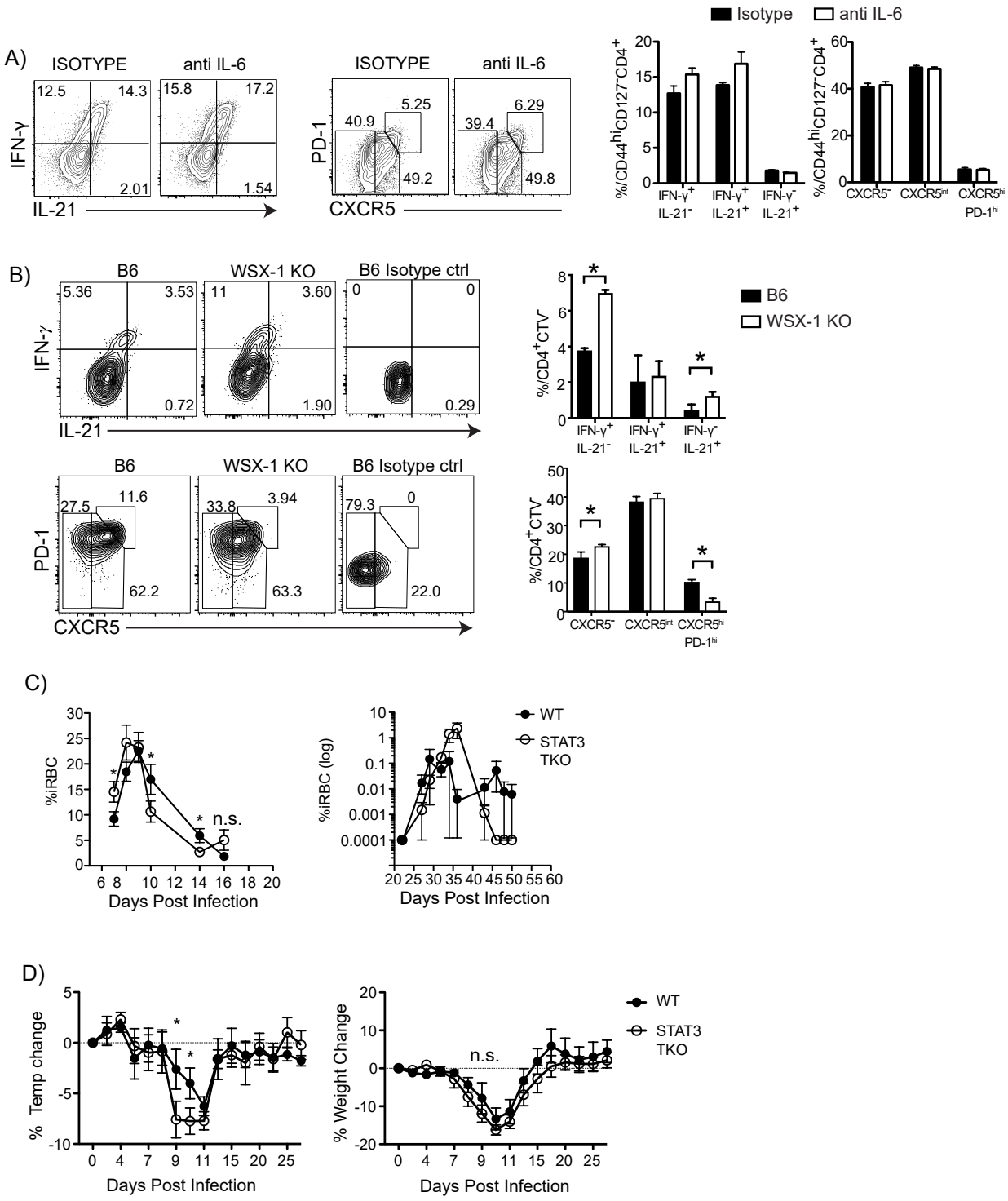

Figure S6. WSX-1 deficiency increases Th1-like Teff. *Related to Figure 5*. (**A**) C57BL/6J mice (n=5/group) were infected with *P. chabaudi* and treated with anti-IL-6 or isotype control antibody. Expression of IFN-γ and IL-21, or PD-1 and CXCR5 in Teff at day 7 p.i. in splenocytes from treated animals (**B**) Splenocytes from uninfected WSX-1 KO or C57BL/6J were labeled with cell trace violet (CTV) and adoptively transferred into Thy1.1 congenic mice, which were then infected with *P. chabaudi*. Expression of IFN-γ/IL-21 and PD-1/CXCR5 in CTV$^-$ gated Teff on day 8 p.i. (**C**, **D**) *Stat3*$^{fl/fl}$CD4^{Cre} (TKO) and *Stat3*$^{fl/fl}$ (WT) animals were infected. (**C**) Parasitemia of WT (filled dots) and STAT3 TKO (open circles) animals. (**D**) Temperature and weight loss of WT and STAT3 TKO animals are shown as percentages of starting value. (**A**, **B**) Data representative of 2 experiments, 3-5 mice/group. (**C**, **D**) Data representative of 3 experiments, 3-8 mice/group. Data are represented as mean ± SEM.

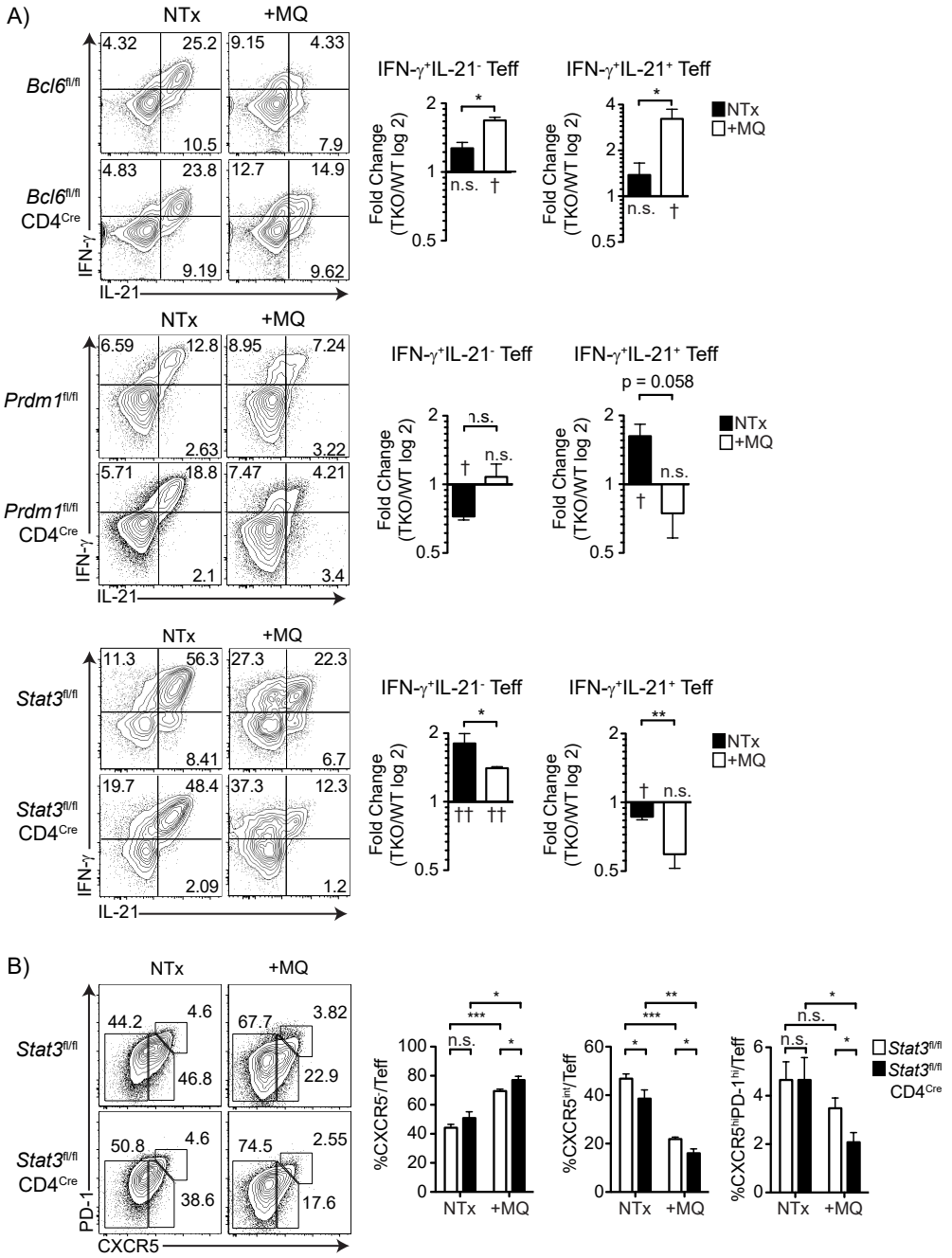

Figure S7. T cell response to long or shortened *P. chabaudi* infection in Bcl6, Blimp-1, and STAT3 TKO mice. *Related to Figure 6*. TKO and WT animals were infected and given mefloquine (+MQ) starting on day 3 p.i. or left untreated (NTx). Splenocytes were harvested and analyzed by flow cytometry at day 7 p.i. (**A**) Contour plots show expression of IFN-γ and IL-21 in Teff. Bar graphs show difference of IFN-γ^+IL-21^- and IFN-γ^+IL-21^+ Teff (average of fold change difference between TKO and WT (log 2 of %TKO/%WT)) from NTx (black bars) or +MQ (white bars) from Bcl6 TKO (top), Blimp-1 TKO (middle), or STAT3 TKO (bottom). (Intracellular cytokine staining in STAT3 TKO was the only one done with commercially prepared secretion inhibitor, hence higher cytokine staining) (**B**) Expression of PD-1 and CXCR5 in Teff from STAT3 TKO and WT mice. Bar graphs show percentages from STAT3 TKO (black bars) or WT (white bars). Data representative of 2 experiments with 3 mice/group. † $p < 0.05$, †† $p < 0.01$ are statistical significance of the difference between WT and TKO mice for each group. Data are represented as mean ± SEM.

Supplemental Information

Transparent Methods

Experimental Model and Subject Details

C57BL/6J (B6), B6.129S1-*Stat3*^{tm1Xyfu}/J (STAT3$^{fl/fl}$), B6.129-*Prdm1*^{tm1Clme}*/J* (Blimp-1$^{fl/fl}$), and B6.129S6-*Tbx21*^{tm1Glm}/J (T-bet KO) mice were purchased from The Jackson Laboratory (Bar Harbor, ME) and bred to B6.Cg-Tg (CD4-Cre)1Cwi N9 mice from Taconic (Hudson, NY). Bcl6$^{fl/fl}$ x CD4-Cre mice (Indiana University School of Medicine, Indianapolis, IN) were bred at UTMB. Six to twelve-week-old animals of both sexes were used for all experiments. All mice were maintained in our specific pathogen free animal facility with *ad libitum* access to food and water. All animal experiments were carried out in compliance with the protocol specifically approved for this study by the University of Texas Medical Branch Institutional Animal Care and Use Committee. Mice were infected i.p. with 10^5 (or 10^7 for re-infection) *P. chabaudi chabaudi* (AS; courtesy of Jean Langhorne (Francis Crick Institute, London, UK)) or 10^5 *P. yoelii* (clone 17XNL; MR4/ATCC) infected red blood cells (iRBCs). Parasites were counted in thin blood smears stained with Giemsa (Sigma, St. Louis, MO) by light microscopy. In some experiments, mice were treated with mefloquine hydrochloride (MQ, 4mg/kg body weight, Sigma, St. Louis, MO) by oral gavage daily five times or until the mice were euthanized. In some experiments (STAT3 TKO) mice were treated with 50 mg/kg body weight per animal of Chloroquine (CQ) in saline (both from Sigma) every other day for a total of three times, starting 10 weeks p.i.

Flow Cytometry and Adoptive Transfer

Single-cell suspensions from spleens were made in Hank's Balanced Salt Solution (Gibco, Life Technologies, Grand Island, NY), with added HEPES (Sigma), followed by red blood cell lysis buffer (eBioscience, San Diego, CA). Multicolor panels including anti-CXCR5 were stained in

PBS + 0.5% BSA + 0.1% sodium azide + 2% Normal Mouse Serum (NMS) and 2% FBS (Sigma, St. Louis, MO). Rat anti-mouse purified CXCR5 (2G8, BDbioscience, San Jose, CA, 1 hr., 4°C) was followed by biotin-conjugated AffiniPure Goat anti-rat (H+L, Jackson ImmunoResearch, West Grove, PA, 30 min, 4°C) followed by Streptavidin-eFluor 450, –PE or –Brilliant Violet 650 (BV650). As described in Crotty et al., the third step included the other antibodies (Crotty, 2014). Combinations of FITC–, phycoerythrin (PE)–, Peridinin Chlorophyll Protein Complex (PerCP)-Cyanine (Cy)5.5, PE/ Cyanine 7 (Cy7), Allophycocyanin (APC) monoclonal antibodies (all from eBioscience, San Diego, CA), and CD127-PE/Cy5, CD44-Brilliant Violet 785 (Biolegend, San Diego, CA) were used. For B cell staining we used B220-PE/Cy5, MHC-II (I-A/I-E)-APC, CD38-PE, GL-7-FITC (all from eBioscience, San Diego, CA). For intracellular staining, total cells were stimulated for 2 h with phorbol myristate acetate (PMA, 50 ng/mL), Ionomycin (500 ng/mL), and Brefeldin A (10 μg/mL, all from Sigma) in complete Iscove's Media 10% FBS, 2mM L-glutamine, 0.5 mM sodium pyruvate, 100 U/ml penicillin, 100ug/ml streptomycin, 50 μM 2-β-Mercaptoethanol (all from Gibco, LifeTechnologies). Figures 4B and S7A STAT3 TKO used GolgiPlug (BDbioscience) in place of Brefeldin A solution. Cells were fixed in 2% paraformaldehyde (Sigma), permeabilized using Permeabilization buffer (Perm buffer, eBioscience) and incubated for 40 minutes with anti-IFN-γ-Brilliant Violet 605 (XMG1.2), T-bet-eFluor 660 or -PerCP-Cy5.5 (eBio4B10, eBioscience), Bcl6-Alexa Fluor 488 or –PE (K112-91), and/or Blimp-1-Alexa Fluor 647 (6D3, BDbioscience). For IL-21 staining, cells were incubated with recombinant mouse IL-21R-Fc chimera (1 μg, 40 min., R&D systems, Minneapolis, MN in Perm buffer), washed twice in Perm buffer followed by AlexaFluor647 goat anti-human IgG $F(ab')_2$ (0.3 μg, 30 min, Jackson ImmunoResearch, West Grove, PA) in Perm buffer. After three washes in Perm buffer, cells were resuspended in FACS buffer and collected on a LSRII Fortessa

at the UTMB Flow Cytometry and analyzed in FlowJo versions 9.4.11, 10.5.3 (TreeStar, Ashland, OR). Compensation was performed in FlowJo using single CD4 stained splenocytes. Cell Trace Violet (CTV, Invitrogen) staining of splenocytes was done in calcium- and magnesium-free PBS at 10^7 cells/ml with 5μM CTV for 10 minutes at 37°C in the dark with periodic shaking, then quenched with Fetal Calf Serum. After washing, 2 x10^6 cells were transferred into each mouse i.p. Reagents are listed in the next table.

REAGENT or RESOURCE	SOURCE	IDENTIFIER
Antibodies		
Purified Rat Anti-Mouse CXCR5 (Clone 2G8)	BD Bioscience	Cat No. 551961, RRID:AB_394302
Biotin-SP (long spacer) AffiniPure Goat Anti-Rat IgG (H+L)	Jackson ImmunoResearch Labs	Cat No. 112-065-167, RRID:AB_2338179
eBioscience™ Streptavidin eFluor™ 450 Conjugate	Thermo Fisher Scientific	Cat No. 48-4317-82, RRID:AB_10359737
PE anti-Streptavidin	Biolegend	Cat No. 410503, RRID:AB_2571914
Brilliant Violet 650™ Streptavidin	Biolegend	Cat No. 405232
PE/Cy7 anti-moue CD279 (PD-1)	Biolegend	Cat No. 109110, RRID:AB_572017
GL-7 Monoclonal Antibody (GL-7), Alexa Fluor 488, eBioscience™	Thermo Fisher Scientific	Cat No. 53-5902-82, RRID:AB_2016717
CD38 (clone HB7), PE, eBioscience™	Thermo Fisher Scientific	Cat No. 12-0388-42, RRID:AB_1518748
CD11a (LFA-1alpha) (clone HI111), FITC, eBioscience™	Thermo Fisher Scientific	Cat No. 11-0119-42, RRID: AB_10596521
PE/Cy5 anti-mouse CD127 (IL-7Rα)	Biolegend	Cat No. 135016, RRID:AB_1937261
Brilliant Violet 785™ anti-mouse/human CD44	Biolegend	Cat No. 103059, RRID:AB_2571953
CD45R (B220) (Clone RA3-6B2), PE-Cyanine5, eBioscience™	Thermo Fisher Scientific	Cat No. 15-0452-82, RRID:AB_468755
MHC Class II (I-A/I-E) (clone M5/114.15.2), APC, eBioscience™	Thermo Fisher Scientific	Cat No. 17-5321-82, RRID:AB_469455
Brilliant Violet 605 anti-mouse IFN-γ	Biolegend	Cat No. 505840, RRID:AB_2734493
Alexa Fluor® 647 AffiniPure F(ab')$_2$ Fragment Goat Anti-Human IgG, F(ab')$_2$ fragment specific	Jackson ImmunoResearch Labs	Cat No. 109-606-006, RRID:AB_2337893
Anti-mouse IL-10 (Clone JES5-16E3), PE, eBioscience™	Thermo Fisher Scientific	Cat No. 12-7101-41, RRID:AB_10669561
Anti-mouse T-bet (Clone eBio4B10(4B10)), eFluor 660, eBioscience™	Thermo Fisher Scientific	Cat No. 50-5825-82, RRID:AB_10596655
Anti-mouse T-bet (Clone eBio4B10(4B10)), PerCP-Cyanine5.5, eBioscience™	Thermo Fisher Scientific	Cat No. 45-5825-82, RRID:AB_953657
Alexa Fluor® 488 Mouse anti-Bcl-6 (Clone K112-91)	BD Bioscience	Cat No. 561524, RRID:AB_10716202

PE Mouse anti-Bcl-6 (Clone K112-91)	BD Bioscience	Cat No. 561522, RRID:AB_10717126
Alexa Fluor® 647 Rat Anti-Blimp-1(Clone 6D3)	BD Bioscience	Cat No. 565002, RRID:AB_2739040
Anti-Mouse IgM (μ-chain specific)-Alkaline Phosphatase antibody produced in goat	Sigma-Aldrich	Cat No. A9688, RRID:AB_258472
Goat Anti-Mouse IgG, Human ads-AP	Southern Biotech	Cat No. 1030-04, RRID:AB_2794293
Goat Anti-Mouse IgG2b-AP	Southern Biotech	Cat No. 1091-04, RRID:AB_2794541
Chemicals, Peptides, and Recombinant Proteins		
Recombinant Mouse IL-21 R Fc Chimera Protein, CF	R&D	Cat No. 596-MR-100
Phorbol Myristate Acetate (PMA)	Sigma	Cat No. P1585
Ionomycin	Sigma	Cat No. I0634
Brefeldin A	Sigma	Cat No. B7651
Protein Transport Inhibitor (Containing Brefeldin A)	BD Bioscience	Cat No. 555029
Ricca Chemical Giemsa Stain	Fisher Scientific	Cat No. 3250-4
Mefloquine hydrochloride	Sigma	Cat No. M2319
Chloroquine diphosphate salt	Sigma	Cat No. C6628
CellTrace™ Violet Cell Proliferation Kit	Invitrogen™	Cat No. C34571
Experimental Models: Organisms/Strains		
C57BL/6J mice	The Jackson Laboratory	Cat No. 000664
B6.129S1-*Stat3*^{tm1Xyfu}/J (STAT3$^{fl/fl}$)	The Jackson Laboratory	Cat No. 016923
B6.129-*Prdm1*^{tm1Clme}/J (Blimp-1$^{fl/fl}$)	The Jackson Laboratory	Cat No. 008100
B6.129S6-*Tbx21*^{tm1Glm}/J	The Jackson Laboratory	Cat No. 004648
B6.Cg-Tg (CD4-Cre)1Cwi N9	Taconics	Cat No. 4196
Bcl6$^{fl/fl}$ x CD4-Cre	(Hollister et al., 2013)	N/A
Parasite Strains		
Plasmodium chabaudi chabaudi (AS)	Jean Langhorne, Crick Institute	N/A
Plasmodium yoelii (Clone 17XNL)	ATCC-BEI	
Software and Algorithms		
FlowJo™ (version 9.4.11)	FlowJo.LLC	https://www.flowjo.com/
FlowJo™ (version 10.5.3)	FlowJo.LLC	https://www.flowjo.com/
Prism	GraphPad	https://www.graphpad.com/scientific-software/prism/
SPICE (version 5.35)	NIAID-NIH	https://niaid.github.io/spice/

ELISA

Serum samples were obtained on the indicated days by bleeding mice from the tail vein under a heat lamp. Nunc-Immuno Plates (MaxiSorp™) were coated with whole freeze-thaw parasite lysate (transfer from N_2(l) to 37°C, 4-5 times (Guthmiller et al., 2017). Plates were blocked with 2.5% BSA + 5%FCS in PBS. Bound antibody was detected using Alkaline Phosphatase (AP)-conjugated goat anti-mouse IgM (Sigma), IgG and IgG2b (Southern Biotech, Brimingham, AL) which was revealed with a 4-Nitrophenyl phosphate disodium salt hexahydrate (PNPP, Sigma) solution (1 mg/ml). Plates were analyzed with a FLUOstar Omega plate reader (BMG Labtech, Cary, NC).

Statistics

Statistical analysis was performed in Prism (GraphPad, La Jolla, CA) using Student's *t*-test. $p < 0.05$ was accepted as a statistically significant difference, * $p \leq 0.05$, ** $p \leq 0.01$, *** $p \leq 0.001$, **** $p \leq 0.001$. Boolean gating analysis and Pie graphs were performed in SPICE software version 5.35 (http://exon.niaid.nih.gov/spice/).

Supplemental References

Hollister, K., Kusam, S., Wu, H., Clegg, N., Mondal, A., Sawant, D.V., and Dent, A.L. (2013). Insights into the role of Bcl6 in follicular Th cells using a new conditional mutant mouse model. J Immunol *191*, 3705-3711.